JOC The Journal of Organic Chemistry

Article

pubs.acs.org/joc

Review of Rate Constants and Exploration of Correlations of the Halogen Transfer Reaction of Trisubstituted Carbon-Centered Radicals with Molecular Halogens

Marvin L. Poutsma*

Chemical Sciences Division, Oak Ridge National Laboratory, P.O. Box 2008, Oak Ridge, Tennessee 37831-6197, United States

Supporting Information

ABSTRACT: Rate constants for the reaction ($R'_3C^\bullet + X_2 \rightarrow R'_3CX + X^\bullet$; X = F, Cl, Br, I) are reviewed. Because of curved Arrhenius plots and negative E_X values, empirical structure−reactivity correlations are sought for log $k_{X,298}$ rather than E_X. The well-known poor correlation with measures of reaction enthalpy is demonstrated. The best quantitative predictor for $R'_3C^\bullet$ is $\sum\sigma_p$, the sum of the Hammett σ_p constants for the three substituents, R′. Electronegative substituents with lone pairs, such as halogen and oxygen, thus appear to destabilize the formation of a polarized prereaction complex and/or TS ($^{\delta+}$R- - -X- - -$X^{\delta-}$) by σ inductive/field electron withdrawal while simultaneously stabilizing them by π resonance electron donation. The best quantitative predictor of the reactivity order of the halogens, $I_2 > Br_2 \gg Cl_2 \approx F_2$, is the polarizability of the halogen, $\alpha(X_2)$. For the data set of 60 rate constants which span 6.5 orders of magnitude, a modestly successful correlation of log $k_{X,298}$ is achieved with only two parameters, $\sum\sigma_p$ and $\alpha(X_2)$, with a mean unsigned deviation of 0.59 log unit. How much of this residual variance is the result of inaccuracies in the data in comparison with oversimplification of the correlation approach remains to be seen.

$R'_3C^\bullet + X_2 \rightarrow R'_3CX + X^\bullet$

$\log k_{X,298} = -(12.45\pm0.27) - (4.18\pm0.28)\,\Sigma\sigma_p + (0.189\pm0.043)\,\alpha(X_2)$

MUD = 0.59 log units

INTRODUCTION

Free-radical halogenation of organics typically occurs by alternating chain steps. The kinetics of the first, to generate $R^\bullet$ either by hydrogen transfer from RH to $X^\bullet$ (eq 1a) or addition to an unsaturated linkage (eq 1b), have received much more attention than those of the second, halogen transfer from X_2 to $R^\bullet$ to generate the RX product (eq 2). We explore herein empirical structure−reactivity relationships for $k_X(R^\bullet)$. The ability to estimate unknown $k_X(R^\bullet)$ values would be especially valuable for chain reactions in which halogen transfer competes with radical rearrangement or capture by other reagents such as O_2. To avoid confusion, we use "R" to indicate the radical itself and "R‴" for substituents on the radical center, even though these need not be C-centered.

$$X^\bullet + R^1R^2R^3C{-}H \xrightarrow{k_H} X{-}H + R^1R^2R^3C^\bullet\ (R^\bullet) \qquad (1a)$$

$$X^\bullet + R^1R^2C{=}CR^3R^4 \xrightarrow{k_{add}} XR^1R^2CCR^3R^{4\bullet}\ (R^\bullet) \qquad (1b)$$

$$R^\bullet + X{-}X \xrightarrow{k_X(R^\bullet)} R{-}X + X^\bullet \qquad (2)$$

BACKGROUND

Rate Constant Determination Methods. We emphasize real-time measurements of $k_X(R^\bullet)$ or of ratios that can be anchored to other real-time measurements, and we include values deduced from data fitting to complex mechanisms only as a last resort. Four generic methods have been used (along with several more specific methods for individual cases that will be cited below). The most common uses a mixture of a photolabile precursor of $R^\bullet$, a variable excess of X_2, and an inert diluent to rapidly thermalize $R^\bullet$ in a temperature-controlled flow cell. Pulsed laser photolysis (PLP) generates $R^\bullet$ in a time period that is short in comparison with the half-life of its decay. Time-resolved monitoring of the decay of $R^\bullet$ (and/or formation of RX) is carried out by an appropriate rapid spectroscopy. The initial concentration of $R^\bullet$ is kept low enough that its combination is slow compared with step 2 which, with an excess of X_2, occurs under pseudo-first-order conditions. The rate constant is then $k_{exp} = k_w + k_X(R^\bullet)[X_2]$, where k_w contains all first-order decay pathways such as wall reactions, and a plot of k_{exp} vs $[X_2]$ gives $k_X(R^\bullet)$. The dominant embodiment of this method coupled the reactor through a pinhole leak into the source of a photoionization mass spectrometer (PIMS) for detection.[1] PLP has also been coupled with other time-resolved spectroscopy such as IR emission from the excited C−H stretching mode of the RX product,[2,3] deconvoluted UV spectra of the evolving mixture of $R^\bullet$ and RX,[4] or laser-induced fluorescence of $R^\bullet$.[5]

In a second method, $R^\bullet$ is continuously generated in the presence of a mixture of X_2 and a competitive radical capture agent Y such as O_2, NO, or HX. The ratio of halogenated to diverted products as a function of $[X_2]/[Y]$ gives k_X/k_Y where k_Y is the rate constant for the competitive reaction. $k_X(R^\bullet)$ can be obtained if k_Y is known from separate time-resolved measurements. We use the shorthand "k_X/k_Y−k_Y" for this approach. For the common use of $Y = O_2$, low enough temperature and high enough pressure are chosen that the peroxy radical formed is thermalized and captured before reversal can occur. A complication is that O_2 addition is often pressure-dependent so that care must be taken that the T−p conditions of the competition

Received: November 8, 2011
Published: February 27, 2012

   dx.doi.org/10.1021/jo2023075 | J. Org. Chem. 2012, 77, 2619−2636

experiment match those of the determination of k_{O_2} (e.g., see refs 6 and 7). Second, the oxidation product(s) have not always been characterized but have simply been equated to the growing discrepancy between [R• consumed] and [RX formed] as $[O_2]$ increases.

In a third method, photoinitiated substitution of RH (step 1a) or addition to an olefin (eq 1b) is carried out under parallel steady-state and intermittent (rotating sector) illumination conditions. If the substrate concentrations are chosen such that $[R^\bullet] \gg [X^\bullet]$ at steady state, termination of the chain reaction is dominated by self-reaction of R• with rate constant k_t. Since the overall steady-state rate constant has the functional form $k_{exp} = f(k_X(R^\bullet), k_t)$ while the intermittent illumination mode allows an absolute determination of k_t, k_{exp} can be deconvoluted to give the desired $k_X(R^\bullet)$.

Finally, the very low pressure reactor (VLPR or VLPΦ) method has been used in which the yields of microwave-induced or photoinduced products effusing from a very low pressure Knudsen cell are determined by mass spectrometry; their variation as a function of the in-flow rate of X_2 and of the escape aperture size allows separation of k_w and $k_X(R^\bullet)$.[8,9] However, the values obtained often tend to be inconsistent with those from other methods (see below), and such data for $k_X(R^\bullet)$ are therefore used sparingly herein.

Rate Constants for Chlorine Transfer. The kinetic database is most extensive for chlorine transfer. Experimental gas-phase data for $k_{Cl}(R^\bullet)$ are collected in Table 1.[2−40] Structures labeled with simple numerals result from single reported measurements or from fits to multiple measurements (see text); such multiple measurements are indicated by the same numeral but with an alphabetic suffix added. Only the numerals without letter suffixes indicate the values of $k_{Cl,298}(R^\bullet)$ used for regression analyses. The majority have been obtained from the PLP/PIMS method,[10−12,18−20,22,30,39] along with several from the $k_{Cl}/k_{O_2}-k_{O_2}$ method[6,7,13−17,23,24,33−36,40] and from the rotating sector method.[21,25−29] Note that the substituents on the radical center are heavily weighted toward alkyl groups and halogen atoms, with limited representation from other heteroatoms (a few O and S but no N) or carbon-centered substituents such as carbonyl. To obtain even these few, more indirect methods and kinetic assumptions were often necessary.

As we move in Table 1 from the least to the most reactive radicals, not only does the Arrhenius E decrease as expected, but for the most reactive cases it becomes negative, especially at lower temperatures; i.e., many of the Arrhenius plots show significant curvature or even minima. Hence, several of the cases in Table 1 are presented in three-parameter rather than the usual two-parameter Arrhenius form. This behavior will be briefly reviewed for some representative cases, especially those for which there have been measurements for the same radical from different research groups as an indicator of data consistency.

An early PLP/PIMS study of methyl (**1b**)[11] gave a small positive E value (296−712 K), but a recent extension of the same method to lower T (188−496 K) (**1a**)[10] revealed a minimum near 273 K and a small negative E value at still lower temperature. A single measurement at 298 K (**1c**)[2] by monitoring the IR emission from the excited C−H stretch of the CH_3Cl product was fully consistent. (This study indicated that approximately half the energy available from the highly exothermic chlorine transfer (see below) goes into product vibration and that reaction in the absence of an inert buffer gas is promoted by translational excitation of methyl, suggestive of at least a small barrier.) We combined these three data sources to give the three-parameter fit shown as **1** in Figure S-1 (Supporting Information). However, a VLPR value at 298 K (**1d**)[8] was 2-fold greater than this regression line. While the temperature dependence is thus complex, note that the total absolute change in $k_{Cl}(CH_3^\bullet)$ is only slightly more than 2-fold for a 500 K change in temperature.

In the same PLP/PIMS studies, ethyl was first reported (**2a**)[11] to show a very small negative E (295−498 K) while the extension to lower T (190−359 K) (**2b**)[12] gave an even more negative E and rate constant values that were systematically somewhat lower at higher temperatures, for reasons unknown to the authors. These two data sets are shown in Figure S-2, along with two measurements at 298 K by different methods. A $k_{Cl}/k_{O_2}-k_{O_2}$ value (**2c**)[6,7] is consistent and is included in our three-parameter fit (**2**). However, a VLPR value (**2d**),[8] in contrast to the positive displacement for methyl (Figure S-1), is over an order of magnitude lower than the other data and is again not included in our fit.

The values of $k_{Cl}(R^\bullet)$ for the series methyl (**1b**), ethyl (**2a**), isopropyl (**6**), and *tert*-butyl (**7**) from the same PLP/PIMS study[11] and T range (298−498 K) are shown in Figure S-3 with linear least-squares fits. The E values are all small (Table 1) but not monotonic, ranging from slightly positive for methyl to slightly negative for ethyl to even slightly more negative for isopropyl but then to essentially zero for *tert*-butyl. The primary radicals ethyl (**2**) (Figure 2), *n*-propyl (**3**),[12] and *n*-butyl (**4a**,**b**) (essentially identical values by two different methods)[12−14] all show slightly negative E values and only a very small successive 1.2-fold increase along this series of increasing radical size. However, this "size effect" is reversed for the secondary radicals isopropyl (**6**)[11] and *sec*-butyl (**5**).[13,14] More likely the rate constants for a given alkyl radical class are independent of size within experimental error.

Three data sets for chloromethyl, **9a**,[18] **9b**,[19] and **9c**,[20] all used the PLP/PIMS method and together cover a very large T range (201−873 K). There is good agreement in the overlap regions, and again the combined Arrhenius plot shown in Figure S-4 shows distinct curvature. The regression line we chose (**9**) is the composite of Rissanen and co-workers.[20] Parallel data for dichloromethyl (**10**)[18] were originally expressed as $(8.6 \times 10^{-13}) \exp(-10.3/RT)$ but later[19] as $(1.30 \times 10^{-20}) T^{2.5} \exp(+0.30/RT)$; in our hands, it is somewhat better represented by **10**. The curvature shown in Figure S-4 is minor, although the data do not extend to as low T as do those for chloromethyl. From the same method but limited to high T (667−873 K), the value for trichloromethyl[19] is shown as **11a**. (An earlier single value at 693 K[22] was 1.8-fold greater than predicted by this correlation line.) A second data set for much lower T (303−425 K) (**11**) from the rotating sector method[21] showed negligible curvature. As shown in Figure S-4, these data sets are somewhat inconsistent unless there is curvature in the intermediate temperature region; we have used the latter because the former, which would give a value ∼1 log unit lower at 298 K, would require a dangerously long temperature extrapolation. For context, the data regression for the parent methyl (**1**) from Figure S-1 is repeated in Figure S-4.

For 1-chloroethyl, a T-dependent set (**27b**)[20] by the PLP/PIMS method is shown in Figure S-5 along with a single value at 298 K (**27a**)[30] by the same method and a single value at 298 K (**27c**)[9] by the VLPR method. The latter again appears to be an outlier. Given the opposite disparities between VLPR results and PLP/PIMS results for methyl and ethyl (see above) and this even greater disparity for 1-chloroethyl, we view results

dx.doi.org/10.1021/jo2023075 | J. Org. Chem. 2012, 77, 2619−2636

Table 1. Values of $k_{Cl}(R^{\bullet})$[a]

no.	R$^{\bullet}$	A[b]	n	E[b]	$k_{Cl,298}$[b]	T range[b]	method[c]	ref
1a	CH_3•	9.73×10^{-20}	2.52	−5.52	1.55×10^{-12}	188−496	PLP; PIMS of radical	10
1b	$CH_3^{\bullet}$	5.01×10^{-12}	0	2.22	2.04×10^{-12}	296−712	PLP; PIMS of radical	11
1c	$CH_3^{\bullet}$				1.54×10^{-12}	298	PLP; IR emission from product	2
1	$CH_3^{\bullet}$	2.56×10^{-18}	2.05	−4.24	1.67×10^{-12}	188−712	fit of **1a−c**	
2a	$CH_3CH_2^{\bullet}$	1.26×10^{-11}	0	−1.26	2.10×10^{-11}	295−498	PLP; PIMS of radical	11
2b	$CH_3CH_2^{\bullet}$	2.80×10^{-7}	−1.73	0	1.47×10^{-11}	190−359	PLP; PIMS of radical	12
2c	$CH_3CH_2^{\bullet}$				1.65×10^{-11}	298	$k_{Cl}/k_{O_2}-k_{O_2}$	6, 7
2	$CH_3CH_2^{\bullet}$	1.85×10^{-19}	2.61	−8.38	1.56×10^{-11}	190−498	fit of **2a−c**	
3	$CH_3CH_2CH_2^{\bullet}$	1.46×10^{-7}	−1.57	0	1.90×10^{-11}	204−363	PLP; PIMS of radical	12
4a	$CH_3CH_2CH_2CH_2^{\bullet}$	1.74×10^{-5}	−2.38	0	2.25×10^{-11}	202−359	PLP; PIMS of radical	12
4b	$CH_3CH_2CH_2CH_2^{\bullet}$				2.33×10^{-11}	296	$k_{Cl}/k_{O_2}-k_{O_2}$	13, 14, 40[d]
4	$CH_3CH_2CH_2CH_2^{\bullet}$	1.74×10^{-5}	−2.38	0	2.30×10^{-11}	202−359	**4a,b** essentially identical	
5	$CH_3CH_2(CH_3)CH^{\bullet}$				4.76×10^{-11}	296	$k_{Cl}/k_{O_2}-k_{O_2}$	13, 14, 40[d]
6	$(CH_3)_2CH^{\bullet}$	2.51×10^{-11}	0	−2.03	5.70×10^{-11}	298−498	PLP; PIMS of radical	11
7	$(CH_3)_3C^{\bullet}$	3.98×10^{-11}	0	−0.04	4.04×10^{-11}	298−498	PLP; PIMS of radical	11
8	$F_3C^{\bullet}$				3.50×10^{-14}	296	$k_{Cl}/k_{O_2}-k_{O_2}$; $k_{Cl}/k_{NO}-k_{NO}$	15−17[e]
9a	$ClCH_2^{\bullet}$	1.50×10^{-12}	0	4.09	2.88×10^{-13}	295−719	PLP; PIMS of radical	18
9b	$ClCH_2^{\bullet}$	4.56×10^{-12}	0	8.93	1.24×10^{-13}	511−873	PLP; PIMS of radical	19
9c	$ClCH_2^{\bullet}$	1.77×10^{-22}	3.26	−6.43	2.76×10^{-13}	201−363	PLP; PIMS of radical	20
9	$ClCH_2^{\bullet}$	2.96×10^{-20}	2.52	−4.36	2.96×10^{-13}	201−873	fit of **9a−c**	20
10	$Cl_2CH^{\bullet}$	1.32×10^{-20}	2.50	0.43	1.70×10^{-14}	357−719	PLP; PIMS of radical; see text	18
11	$Cl_3C^{\bullet}$	9.12×10^{-13}	0	20.92	1.96×10^{-16}	303−425	rotating sector on $Cl_3CH + Cl_2$	21
12	$BrCH_2^{\bullet}$	1.20×10^{-12}	0	2.40	4.55×10^{-13}	295−524	PLP; PIMS of radical	18
13	$ICH_2^{\bullet}$	1.20×10^{-12}	0	0.80	8.69×10^{-13}	295−524	PLP; PIMS of radical	18
14	$FCl_2C^{\bullet}$	1.38×10^{-12}	0	14.00	4.85×10^{-15}	435−693	PLP; PIMS of radical	22
15	$F_2ClC^{\bullet}$	1.29×10^{-12}	0	8.00	5.10×10^{-14}	376−626	PLP; PIMS of radical	22
16	$BrClCH^{\bullet}$	5.83×10^{-20}	2.30	0.30	2.53×10^{-14}	348−828	PLP; PIMS of radical	19
17	$(CF_3)FCH^{\bullet}$				1.43×10^{-14}	296	$k_{Cl}/k_{O_2}-k_{O_2}$	23, 24[f]
18	$(CF_3)Cl_2C^{\bullet}$	2.09×10^{-12}	0	24.36	1.12×10^{-16}	314−350	rotating sector on $(CF_3)Cl_2CH + Cl_2$	25
19	$(CFCl_2)FClC^{\bullet}$	7.95×10^{-13}	0	20.12	2.36×10^{-16}	303−363	rotating sector on $CFCl{=}CFCl + Cl_2$	26
20	$(CCl_3)ClCH^{\bullet}$	3.72×10^{-13}	0	19.26	1.57×10^{-16}	349−404	$(CCl_3)ClCH_2 + Cl_2$; k_t assigned	27, 28
21	$(CCl_3)Cl_2C^{\bullet}$	3.31×10^{-13}	0	22.60	3.61×10^{-17}	298−321	rotating sector on $CCl_2{=}CCl_2 + Cl_2$	29[g]
22	$(CHCl_2)ClCH^{\bullet}$	1.05×10^{-12}	0	11.30	1.10×10^{-14}	298−321	rotating sector on $CHCl{=}CHCl + Cl_2$	29[g]
23	$(CHCl_2)Cl_2C^{\bullet}$	5.25×10^{-13}	0	21.30	9.69×10^{-17}	298−321	rotating sector on $CHCl{=}CCl_2 + Cl_2$	29[g]
24	$(CH_2Cl)CH_2^{\bullet}$	4.17×10^{-12}	0	4.18	7.70×10^{-13}	298−321	rotating sector on $CH_2{=}CH_2 + Cl_2$	29[g]
25	$(CH_2Cl)ClCH^{\bullet}$	1.05×10^{-12}	0	3.77	2.29×10^{-13}	298−321	rotating sector on $CH_2{=}CHCl + Cl_2$	29[g]
26	$(CH_2Cl)Cl_2C^{\bullet}$	1.05×10^{-12}	0	17.20	1.01×10^{-15}	298−321	rotating sector on $CH_2{=}CCl_2 + Cl_2$	29[g]
27a	$(CH_3)ClCH^{\bullet}$				4.37×10^{-12}	298	PLP; PIMS of radical	30
27b	$(CH_3)ClCH^{\bullet}$	3.69×10^{-20}	2.52	−9.46	2.89×10^{-12}	191−363	PLP; PIMS of radical	20
27	$(CH_3)ClCH^{\bullet}$	5.57×10^{-17}	1.43	−6.92	3.14×10^{-12}	191−363	fit of **27a,b**	
28a	$(CH_3)Cl_2C^{\bullet}$	1.10×10^{-26}	4.30	−15.0	2.04×10^{-13}	414−873	PLP; PIMS of radical	19
28b	$(CH_3)Cl_2C^{\bullet}$	5.42×10^{-13}	−0.26		1.23×10^{-13}	240−363	PLP; PIMS of radical	20
28	$(CH_3)Cl_2C^{\bullet}$	1.17×10^{-22}	3.07	−8.07	1.20×10^{-13}	240−873	fit of **28a,b**	20
29	$HSCH_2^{\bullet}$				2.60×10^{-13}	298	PLP; IR emission from HCl[h]	20[h]
30	$CH_3SCH_2^{\bullet}$				7.12×10^{-12}	298	discharge on $(CH_3)_2S$; MS of product[i]	31
31	$HOCH_2^{\bullet}$				2.90×10^{-11}	298	recommended value[j]	30
32a	$CH_3OCH_2^{\bullet}$	1.80×10^{-11}	0	−2.99	6.02×10^{-11}	220−357	PLP; deconvolution of UV spectra	4
32b	$CH_3OCH_2^{\bullet}$				1.00×10^{-10}	298	$k_{Cl}/k_{O_2}-k_{O_2}$	33, 34[k]
32	$CH_3OCH_2^{\bullet}$	2.10×10^{-11}	0	−2.72	6.30×10^{-11}	220−357	fit of **32a,b**	
33	$C_2H_5C(=O)CH_2^{\bullet}$				2.70×10^{-14}	298	$k_{Cl}/k_{O_2}-k_{O_2}$[l]	35
34	$CH_3C(=O)CH^{\bullet}(CH_3)$				1.13×10^{-14}	298	$k_{Cl}/k_{O_2}-k_{O_2}$[l]	35
35	$C_2H_5C(=O)CH^{\bullet}(CH_3)$				1.85×10^{-14}	298	$k_{Cl}/k_{O_2}-k_{O_2}$[l]	36
36	$C_6H_5CH_2^{\bullet}$	5.71×10^{-12}	0	3.68	1.29×10^{-12}	295−384	PLP; LIF of radical	5
1d	$CH_3^{\bullet}$[m]				3.40×10^{-12}	298	VLPR on $Cl/C_2H_6/Cl_2$ system; side reacn	8
2d	$CH_3CH_2\bullet$[m]				1.05×10^{-12}	298	VLPR on $Cl/C_2H_6/Cl_2$ system	8
8a	$F_3C^{\bullet}$[m]	4.47×10^{-12}	0	15.0	1.05×10^{-14}	487−693	PLP; PIMS of radical	22
8b	$F_3C^{\bullet}$[m]	1.28×10^{-11}	0	15.06	2.93×10^{-14}	400−500	k_{Cl} referenced to k_{HCl}, then to k_t	37, 38
27c	$(CH_3)ClCH^{\bullet}$[m]				1.70×10^{-13}	298	VLPR on $C_2H_5Cl + Cl_2$; prelim value	9

dx.doi.org/10.1021/jo2023075 | J. Org. Chem. 2012, 77, 2619−2636

Table 1. continued

no.	R•	A^b	n	E^b	$k_{Cl,298}{}^b$	T range^b	method^c	ref
11a	$Cl_3C^{\bullet m}$	8.40×10^{-13}	0	25.0	3.48×10^{-17}	667−873	PLP; PIMS of radical	19
37	$H_2C{=}CHCH_2^{\bullet m}$	1.55×10^{-11}	0	18.0	1.08×10^{-14}	487−693	PLP; PIMS of radical	39
38	$HC{\equiv}CCH_2^{\bullet m}$	2.75×10^{-11}	0	28.0	3.40×10^{-16}	525−693	PLP; PIMS of radical	39

[a] $k_{Cl} = AT^n \exp(-E/RT)$, $A \exp(-E/RT)$, or AT^n. Entries with only $k_{Cl,298}$ report no other temperature data. For cases with multiple reports, each is indicated by a numeral and letter designation while the selected data (see text), used in the correlations, is indicated by the numeral only. [b] A and $k_{Cl,298}$ in cm^3 molecule^{-1} s^{-1}, E in kJ/mol, and T in K. [c] See text for details. [d] $k_{Cl}/k_{O_2} = 3.1$ at 296 K for 1-butyl and 2.8 for 2-butyl; $k_{O_2} = 7.5 \times 10^{-12}$ for 1-butyl and 1.7×10^{-11} at 300 K for 2-butyl. [e] Values of k_{Cl}/k_{O_2} and k_{Cl}/k_{NO} determined in same pressure range as the values of k_{O_2} and k_{NO}; value given is average of 3.3×10^{-14} and 3.7×10^{-14} from the two competitors. [f] $k_{Cl}/k_{O_2} = 1.63 \times 10^{-1} \exp(-7.82/RT)$; $k_{O_2} = 2.1 \times 10^{-12}$ at 298 K. [g] See text. [h] Monitoring the complex time evolution of emission from HCl allowed mathematical deconvolution of a fast chain with $CH_3S^\bullet$ and a slow chain with $HSCH_2^\bullet$. [i] Some fitting of other rate constants involved. [j] PLP of Cl_2/CH_3OH with resonance fluorescence detection of a biexponential $Cl^\bullet$ decay and computer simulation; compared with k_{Cl}/k_{O_2}−k_{O_2}. [k] $k_{Cl}/k_{O_2} = 9$; $k_{O_2} = 1.09 \times 10^{-11}$. [l] k_{O_2} assumed to be equal to that for $CH_3C(=O)CH_2^\bullet$. [m] Not used in correlations; see text.

from the VLPR method with suspicion and exclude them from our regressions (see Table 1). Hence, that shown (**27**) includes only the first two sources. For 1,1-dichloroethyl in nonoverlapping T ranges, there are two data sources (**28a**[19] and **28b**[20]). The joint regression line shown in Figure S-5 shows a shallow minimum. For context, the data regression for the parent ethyl (**2**) from Figure S-2 is repeated in Figure S-5.

The T-dependent value for methoxymethyl (**32a**)[4] was only slightly altered (**32**) by including one data point (**32b**) from another group.[33] Although the range (220−357 K) was rather small to detect curvature, the former data set again indicated a negative E value. The data for polychloroethyl radicals **21**−**26** is based on rotating sector studies of addition of Cl_2 to polychloroolefins.[29] For the unsymmetrical olefins (**23**, **25**, and **26**), we have assumed that addition of $Cl^\bullet$ occurs regioselectively at the least substituted carbon. The value for trifluoromethyl (**8**) is the average of the very similar values from the k_{Cl}/k_{O_2}−k_{O_2} and k_{Cl}/k_{NO}−k_{NO} approaches at 298 K (**13**).[15−17] It is ∼2-fold larger than a value that can be extrapolated from data at 400−500 K (**8b**)[37] for the ratio of k_{Cl}/k_{HCl} for the hydrogen transfer from HCl, with the latter secondarily referenced[37] to k_t for radical combination;[38] it is ∼3-fold larger than that obtained from an even longer extrapolation of the Arrhenius expression determined (487−693 K) (**8a**)[22] by the PLP/PIMS method; it is not clear whether these modest differences result from experimental uncertainty or from minor curvature in the Arrhenius plot. The fact that benzyl (**36**)[5] appears to be 120-fold more reactive at 298 K than allyl (**37**),[39] although admittedly involving a long T extrapolation for the latter, seems unusual, and an error in one of these values is suspected.

The final seven entries of Table 1 are not used in correlations below for $k_{Cl,298}$, because they were derived from suspect VLPR studies (see above) or would involve a very long T extrapolation.

Rate Constants for Bromine Transfer. The kinetic database for bromine transfer is less extensive than that for chlorine transfer, and the radicals studied do not totally coincide. Experimental gas-phase data for $k_{Br}(R^\bullet)$ are collected in Table 2.[2,37,38,41−49] There are several examples of the PLP/PIMS method, but the rotating sector and k_X/k_{O_2}−k_{O_2} methods have not been applied to Br_2. The VLPΦ method that uses infrared multiphoton dissociation (IRMPD) to generate radicals[45,46] gave values consistent with those from other methods for the overlap case of trifluoromethyl, and hence these data are included, in contrast to the case of Cl_2. The data set in Table 2 is even more heavily weighted toward alkyl and halogen substituents than was the set for $k_{Cl}(R^\bullet)$ in Table 1, and it unfortunately contains no cases with O, S, or carbonyl functionalities. Hence, it is a poorer testing ground for structure−reactivity correlations.

For cases where the T dependence was determined, the *majority* of E_{Br} values are negative, with positive values for only the slowest cases such as trifluoromethyl (**8′**), trichloromethyl (**11′**), and propargyl (**38′**). Examples of distinct Arrhenius curvature have not been reported, but most of the T ranges are more limited than for k_{Cl}. For cases for which multiple measurements are available for the same radical from different research groups, our choices of k_{Br} to be used for correlations will be briefly reviewed.

Results from a typical early study of methyl (**1a′**)[41] by the PLP/PIMS method (296−532 K) and a very recent study (**1b′**)[42] by monitoring resonance fluorescence from $Br^\bullet$ over a somewhat lower T range (224−358 K) overlap well, and the combined two-parameter Arrhenius regression is given as **1′**. Although these two combined data sets could be fit slightly better by $(4.05 \times 10^{-13})T^{0.55} \exp(+3.74/RT)$, the curvature was minimal at best and highly influenced by two extreme data points. A single measurement at 298 K (**1c′**)[2] from following the IR emission from the C−H stretch of the CH_3Br product was almost 2-fold slower and was not included in the Arrhenius regressions.

There are three quite similar values of $k_{Br,298}$ for trifluoromethyl from three different methods: the PLP/PIMS method (**8b′**),[43] the time-resolved IR monitoring of the decaying radical (**8b′**),[44] and VLPΦ measurements (the average of two values from different aperture sizes that differed by a factor of 1.4) (**8c′**).[45] We used the average for **8′**. An early Arrhenius expression was obtained by a less direct method[37] in which (a) formation of $CF_3^\bullet$ in varying mixtures of Br_2 and HCl gave the ratio k_{Br}/k_{HCl} (where k_{HCl} is the rate constant for hydrogen transfer from HCl) at 450−600 K, (b) formation of $CF_3^\bullet$ in varying amounts of HCl alone gave the ratio $k_{HCl}/k_t^{1/2}$ (where k_t is the rate constant for radical combination), and (c) k_t was determined independently. Using the then extant value of k_t with these combined ratios gave a very similar value; however, using the more current values of k_t[38] gives a value only half as large. Given the indirectness of the method, the length of the T extrapolation, and the uncertainty in k_t, we chose not to include this value in our average.

The T-dependent value from the PLP/PIMS method for allyl (**37a′**)[48] was in full agreement with a single measurement at 298 K from the variant of using IRMPD rather than UV as the

dx.doi.org/10.1021/jo2023075 | J. Org. Chem. 2012, 77, 2619−2636

Table 2. Values of $k_{Br}(R^{\bullet})$[a]

no.	R$^{\bullet}$	A[b]	E[b]	$k_{Br,298}$[b]	T range[b]	method[c]	ref
1a′	$CH_3^{\bullet}$	2.00×10^{-11}	−1.63	3.86×10^{-11}	296−532	PLP; PIMS of radical	41
1b′	$CH_3^{\bullet}$	1.83×10^{-11}	−2.10	4.26×10^{-11}	224−358	PLP; resonance fluorescence of Br$^{\bullet}$	42
1c′	$CH_3^{\bullet}$			2.01×10^{-11}	298	PLP; IR emission from product	2
1′	$CH_3^{\bullet}$	1.63×10^{-11}	−2.31	4.14×10^{-11}	224−532	fit of **1a′**,**b′**	
2′	$CH_3CH_2^{\bullet}$	2.60×10^{-11}	−3.43	1.04×10^{-10}	298−532	PLP; PIMS of radical	41
6′	$(CH_3)_2CH^{\bullet}$	2.40×10^{-11}	−4.48	1.46×10^{-10}	298−532	PLP; PIMS of radical	41
7′	$(CH_3)_3C^{\bullet}$	2.00×10^{-11}	−4.06	1.03×10^{-10}	300−532	PLP; PIMS of radical	41
8a′	$F_3C^{\bullet}$			1.14×10^{-12}	296	PLP; PIMS of radical	43
8b′	$F_3C^{\bullet}$			1.79×10^{-12}	298	PLP; IR of product	44
8c′	$F_3C^{\bullet}$			1.30×10^{-12}	298	pulsed IRMPD; MS of product; VLPΦ	45
8d′	$F_3C^{\bullet}$	2.04×10^{-12}	2.80	6.59×10^{-13}	450−600	k_{Br}/k_{HCl}−$k_{HCl}/k_t^{1/2}$−k_t absolute	37[d]
8′	$F_3C^{\bullet}$			1.41×10^{-12}	298	av of **8a′**−**c′**	
9′	$ClCH_2^{\bullet}$	4.80×10^{-12}	−2.80	1.49×10^{-11}	296−532	PLP; PIMS of radical	43
10′	$Cl_2CH^{\bullet}$	9.80×10^{-13}	−1.59	1.86×10^{-12}	296−532	PLP; PIMS of radical	43
11′	$Cl_3C^{\bullet}$	2.99×10^{-13}	5.98	2.67×10^{-14}	300−532	PLP; PIMS of radical	47
12′	$BrCH_2^{\bullet}$	5.50×10^{-12}	−3.01	1.85×10^{-11}	299−539	PLP; PIMS of radical	43
13′	$ICH_2^{\bullet}$	7.80×10^{-12}	−3.30	2.96×10^{-11}	304−539	PLP; PIMS of radical	43
14′	$FCl_2C^{\bullet}$	6.40×10^{-13}	−0.42	7.58×10^{-13}	298−532	PLP; PIMS of radical	43
15′	$F_2ClC^{\bullet}$	1.30×10^{-12}	−0.54	1.62×10^{-12}	298−532	PLP; PIMS of radical	43
37a′	$H_2C{=}CHCH_2^{\bullet}$	4.80×10^{-12}	−1.60	9.16×10^{-12}	298−532	PLP; PIMS of radical	48
37b′	$H_2C{=}CHCH_2^{\bullet}$			9.00×10^{-12}	300	pulsed IRMPD; PIMS of radical	49
37′	$H_2C{=}CHCH_2^{\bullet}$	4.86×10^{-12}	−1.55	9.12×10^{-12}	298−532	fit of **37a′**,**b′**	
38′	$HC{\equiv}CCH_2^{\bullet}$	2.80×10^{-12}	2.30	1.11×10^{-12}	296−532	PLP; PIMS of radical	48
39′	$(CF_3)F_2C^{\bullet}$			3.23×10^{-13}	298	pulsed IRMPD; MS of product; VLPΦ	46
40′	$(CF_3CF_2)F_2C^{\bullet}$			4.98×10^{-13}	298	pulsed IRMPD; MS of product; VLPΦ	46

[a] $k_{Br} = A \exp(-E/RT)$. Entries with only $k_{Br,298}$ report no other temperature data. For cases with multiple reports, each is indicated by a numeral and letter designation while the selected data (see text), used in the correlations, is indicated by the numeral only. The numerals correspond to those in Table 1. [b] A and $k_{Br,298}$ in cm^3 molecule^{-1} s^{-1}, E in kJ/mol, and T in K. [c] See text for details. [d] $k_{Br}/k_{HCl} = 13.8 \exp(+4.40/RT)$; $k_{HCl}/k_t^{1/2} = (4.47 \times 10^{-8}) \exp(-5.07/RT)$ cm$^{1/2}$ molecule$^{-1/2}$ s$^{-1/2}$; $k_t = 1.10 \times 10^{-11}$.[38]

pulsing source for radical formation (**37b′**),[49] and we used a combined fit as **37′**.

Rate Constants for Iodine Transfer. We are not aware of any real-time measurements of $k_I(R^{\bullet})$ that do not involve deconvolution of rate constant ratios or sums, and in comparison to chlorine and bromine transfer, these data are even still more limited in scope and often seriously scattered. Key examples of the probably less accurate data are collected in Table 3.[37,40,50−68] For simple alkyl radicals, the E values are systematically negative to an even greater extent than for chlorine or bromine transfer and E is near zero even for the relatively unreactive trifluoromethyl.

For methyl, the k_I/k_{HX}−k_{HX} method dominates in which absolute values of k_{HX} are usually from the PLP/PIMS method (see footnotes to Table 3). Generation of methyl by photolysis of acetone in a mixture of I_2 and HBr gave k_I/k_{HBr},[50] which we combined with either of two very similar k_{HBr} values[51,52] to obtain **1a″** and **b″**. For **1c″** and **d″**, obtaining the k_I/k_{HBr} ratios[53] involved use of methyl iodide instead as the photolytic source of methyl. Thus, the former[50] somewhat lower values may be more reliable than the latter[53] because of improved analytical capability and avoidance of the complication of methyl iodide being both the precursor and a product. Application of the latter procedure[53] with a mixture of I_2 and HI gave a k_I/k_{HI} ratio which we combined with a k_{HI} value[54] to obtain **1e″**. In a variant,[55] only acetone and HI were fed and I_2 accumulated during reaction (formally $CH_3^{\bullet} + HI \rightarrow CH_4 + {}^1/_2\ I_2$); in this case, the Arrhenius plot was curved such that the value extrapolated to 298 K (**1f″**) may be an upper limit. In an alternate to pulsed photolysis, others[56−58] derived the k_I/k_{HI} ratio from steady-state analysis of the kinetics of the thermal $CH_3I + HI \rightarrow CH_4 + I_2$ reaction; combination with the same k_{HI} value gave **1g″**. All these values lie within a factor of <2.5 of each other, centered at $\sim 9 \times 10^{-11}$ at 298 K. (Note that the values estimated in early papers, e.g. 1.3×10^{-12},[56] were much lower because the estimates of k_{HX} used then were lower, since negative E values were not accepted.) In a very different approach, an optoacoustic method[59] applied to the photolysis of R−I involves modulation of the photolysis intensity which leads to a modulation in the heat release from the chemical reactions, with a phase lag in the resulting acoustic response that depends on the kinetics; a small oscillatory change in concentration of reactive radicals, superimposed on a steady-state background, leads to the signal detected. However, the rate constant extracted from the data is the sum $k_{exp} = k_I[I_2] + k_c[I^{\bullet}][M]$, the deconvolution of which required determination of the steady-state concentrations of I$^{\bullet}$ and I_2, which was done separately, and also assignment of $\Delta_r H$ values for the two radical-consuming steps. In contrast to the k_I/k_{HX}−k_{HX} method, the value of $k_{I,298}(CH_3^{\bullet})$ (**1h″**) obtained by this complex protocol was over an order of magnitude smaller, and it was not included in our selected average (**1″**).

Photolysis of methyl ethyl ketone in a mixture of I_2 and HBr analogously gave k_I/k_{HBr} for ethyl,[50] which we combined with k_{HBr} for ethyl[51] to obtain **2a″**. Steady-state analysis of the kinetics of the thermal $C_2H_5I + HI \rightarrow C_2H_6 + I_2$ reaction gave a k_I/k_{HI} ratio[60] which we combined with k_{HI}[54] to obtain **2b″**. These give essentially the same value for $k_{I,298}$, although the Arrhenius expressions are quite different. Photolysis of ethane−I_2−HI mixtures at 297 K allowed extraction of a k_I/k_{HI} ratio[61] which we combined with the same value of k_{HI}[54] to obtain **2c″**.

dx.doi.org/10.1021/jo2023075 | J. Org. Chem. 2012, 77, 2619−2636

Table 3. Values of $k_I(R^\bullet)$[a]

no.	$R^\bullet$	A[b]	E[b]	$k_{I,298}$[b]	T range[b]	method[c]	ref
1a″	$CH_3^\bullet$	3.1×10^{-12}	−7.3	6.1×10^{-11}	353−437	k_I/k_{HBr}−k_{HBr}	50[d]
1b″	$CH_3^\bullet$	4.6×10^{-12}	−6.3	5.9×10^{-11}	353−437	k_I/k_{HBr}−k_{HBr}	50, 52[e]
1c″	$CH_3^\bullet$	1.2×10^{-11}	−5.6	1.1×10^{-10}	256−411	k_I/k_{HBr}−k_{HBr}	53[f]
1d″	$CH_3^\bullet$	1.7×10^{-11}	−4.6	1.1×10^{-10}	188−712	k_I/k_{HBr}−k_{HBr}	52, 53
1e″	$CH_3^\bullet$	2.0×10^{-11}	−4.3	1.1×10^{-10}	356−428	k_I/k_{HI}−k_{HI}	53, 54[g]
1f″	$CH_3^\bullet$	1.1×10^{-11}	−6.6	$<1.6 \times 10^{-10}$	400−570	k_I/k_{HI}−k_{HI}	54, 55[h]
1g″	$CH_3^\bullet$	1.4×10^{-11}	−4.6	9.0×10^{-11}	533−589	k_I/k_{HI}−k_{HI}	54, 56[i]
1h″	$CH_3^\bullet$			5.8×10^{-12}	298	optoacoustic photolysis of CH_3I	59
1″	$CH_3^\bullet$			9.0×10^{-11}		selected from **1a″**−**g″**	
2a″	$CH_3CH_2^\bullet$	1.0×10^{-12}	−13.8	2.6×10^{-10}	328−388	k_I/k_{HBr}−k_{HBr}	50, 51[j]
2b″	$CH_3CH_2^\bullet$	1.7×10^{-11}	−7.0	2.9×10^{-10}	536−576	k_I/k_{HI}−k_{HI}	54, 60[k]
2c″	$CH_3CH_2^\bullet$			1.7×10^{-10}	298	photolysis of C_2H_6−I_2−HI	54, 61[l]
2d″	$CH_3CH_2^\bullet$			1.0×10^{-10}	298	k_I/k_{O_2}−k_{O_2}	40, 62[m]
2e″	$CH_3CH_2^\bullet$			1.6×10^{-12}	298	k_I/k_{NO}−k_{NO}	62, 63[n]
2f″	$CH_3CH_2^\bullet$			5.0×10^{-11}	298	flash photolysis of C_2H_5I; see text	64
2g″	$CH_3CH_2^\bullet$			6.3×10^{-12}	298	optoacoustic photolysis of C_2H_5I	59
2″	$CH_3CH_2^\bullet$			1.7×10^{-10}	298	av of **2a″**−**d″**,**f″**	
8a″	$CF_3^\bullet$	2.4×10^{-12}	0.59	1.9×10^{-12}	∼450[o]	several ratios anchored to k_t^p	37, 65
8b″	$CF_3^\bullet$			2.4×10^{-13}[q]	600−800	kinetic analysis of pyrolysis of CF_3I	67
8″	$CF_3^\bullet$	2.4×10^{-12}	0.59	1.9×10^{-12}	∼450[o]	use **8a″**	
13″	$ICH_2^\bullet$			3.3×10^{-10}	298	optoacoustic photolysis of ICH_2I	59
37″	$CH_2{=}CHCH_2^\bullet$			1.2×10^{-11}	298	k_I/k_{O_2}−k_{O_2}	68[r]

[a] $k_I = A\exp(-E/RT)$. Entries with only $k_{I,298}$ report no other temperature data. For cases with multiple reports, each is indicated by a numeral and letter designation while the selected data (see text), used in the correlations, is indicated by the numeral only. The numerals correspond to those in Table 1. [b] A and $k_{I,298}$ in cm^3 $molecule^{-1}$ s^{-1}, E in kJ/mol and T in K. [c] See text for details. [d] $k_I/k_{HBr} = 2.0\exp(+5.73/RT)$; $k_{HBr} = (1.57 \times 10^{-12})\exp(+1.6/RT)$. [e] $k_{HBr} = (2.3 \times 10^{-12})\exp(+0.6/RT)$. [f] $k_I/k_{HBr} = 7.5\exp(+3.97/RT)$. [g] $k_I/k_{HI} = 4.4\exp(+3.14/RT)$; $k_I = (4.5 \times 10^{-12})\exp(+1.2/RT)$. [h] $k_I/k_{HI} = <2.4\exp(+5.44/RT)$. [i] $k_I/k_{HI} = 3.2\exp(+3.35/RT)$.[57,58] [j] $k_I/k_{HBr} = 0.6\exp(+9.56/RT)$; $k_{HBr} = (1.7 \times 10^{-12})\exp(+4.2/RT)$. [k] $k_I/k_{HI} = 3.8\exp(+3.77/RT)$; $k_{HI} = (4.5 \times 10^{-12})\exp(+3.2/RT)$. [l] $k_I/k_{HI} = 10.3$ at 298 K. [m] $k_{O_2} = 7.8 \times 10^{-12}$. [n] $k_I/k_{NO} = 7$); $k_{NO} = 2.3 \times 10^{-13}$. [o] Approximate center point of several ranges. [p] k_I/k_{HBr}−k_{HBr}/k_{Br}−k_{Br}/k_{HCl}−$k_{HCl}/k_t^{1/2}$−$k_t^{1/2}$; see text. [q] Value at 600−800 K said to be T independent. [r] $k_I/k_{O_2} = 20$ and $k_{O_2} = 6 \times 10^{-13}$.

The increase in the quantum yield of I_2 from photolysis of ethyl iodide by addition of O_2 or NO was interpreted[62] as resulting from competitive capture of ethyl and the ratios k_I/k_{O_2} and k_I/k_{NO} at 298 K were extracted in a pressure range where the competitive combination reactions were second-order. However, combining with presently compiled values for k_{O_2} and k_{NO}[63] gives the very different values of **2d″** and **2e″**. Flash photolysis of ethyl iodide at 298 K with time-resolved spectral monitoring of the I_2 produced showed a distinctive minimum in the $[I_2]$−t profile during the second and third pulses, indicative of a rapid I_2-consuming step, and kinetic modeling[64] suggested the value of **2f″**. Finally, the optoacoustic method[59] again gave a lower value (**2g″**). In summary, the spread in values for ethyl is larger than that for methyl, and we used an arbitrarily selected average of 1.7×10^{-10} (**2″**). Two values for *n*-propyl at 298 K, 0.5×10^{-10} [64] and 1.8×10^{-10},[62] are similar to those assigned for ethyl and are not included in Table 3.

Photolysis of hexafluoroacetone in the presence of competitive pairs of HX and X_2[37,65,66] gave a lengthy series of rate constant ratios for trifluoromethyl that were ultimately anchored to an absolute value of k_t. Thus, $k_I(CF_3^\bullet) = [k_I/k_{HBr}]$-$[k_{HBr}/k_{Br}][k_{Br}/k_{HCl}][k_{HCl}/k_t^{1/2}][k_t^{1/2}] = [4.35\exp(+2983/RT)$ (358−503 K)][0.264 $\exp(-2171/RT)$ (328−607 K)][13.8 $\exp(+4400/RT)$ (451−600 K)][$(3.47 \times 10^4)\exp(-5070/RT$ $cm^{3/2}$ $mol^{-1/2}$ $s^{-1/2}$) (293−478 K)][6.8×10^{12} cm^3 mol^{-1} s^{-1} (T-independent)]$^{1/2}$, where we have altered k_t from that originally used to a more current value (see above)[38,66] and the ΔE values are in cal/mol. In the units used herein and centered on ∼450 K, this product leads to the value given as **8a″**. A very complex steady-state analysis of the pyrolysis of perfluoroalkyl iodides ($R_fI \rightarrow {}^1/_2\ R_f{-}R_f + {}^1/_2\ I_2$) with some input of other rate and equilibrium constants[67] was used to extract a much smaller T-independent value (**8b″**). (The values reported for $C_2F_5^\bullet$, *n*-$C_3F_7^\bullet$, *i*-$C_3F_7^\bullet$, and *n*-$C_4F_9^\bullet$ were smaller still, 1.4×10^{-13}, 5.4×10^{-14}, 1.2×10^{-13}, and 2.1×10^{-14}, respectively.) We have chosen to accept the first value as **8″**.

The optoacoustic method[59] gave a value for iodomethyl (**13″**) that was some 50-fold *greater* than that for ethyl by the same method, which led the authors (not surprisingly) to suspect an unidentified complicating mechanism. Various flash photolyses of 1,5-hexadiene and allyl iodide in the presence of O_2 and I_2, with UV spectroscopic monitoring,[68] allowed the extraction of k_I/k_{O_2}, k_{O_2}, and hence the value shown as **37″** for allyl.

Rate Constants for Fluorine Transfer. The database of rate constants for fluorine transfer is even more sparse than that for iodine transfer and tends to rely on more specialized methods. It is summarized in Table 4.[23,24,40,69−73]

For methyl, pulsed laser photolysis of F_2 in the presence of methane and time-resolved detection of the IR emission from vibrationally excited HF allowed the extraction of both the rate constants for hydrogen and fluorine transfer (**1a‴**).[69] Study of the pre-explosive phase of CH_4−F_2 mixtures at 300−400 K in a small tubular reactor functioning as the source in a molecular beam apparatus with mass spectroscopic detection[70] gave the composite quantities A_oA_F and $E_o + E_F$, where reaction "o" is the proposed initiation step: $CH_4 + F_2 \rightarrow CH_3^\bullet + HF + F^\bullet$.

dx.doi.org/10.1021/jo2023075 | J. Org. Chem. 2012, 77, 2619−2636

Table 4. Values of $k_F(R^\bullet)$[a]

no.	R$^\bullet$	A[b]	E[b]	$k_{1,298}$[b]	T range[b]	method[c]	ref
1a‴	$CH_3^\bullet$	7.0×10^{-12}	4.07	1.35×10^{-12}	139–294	PLP of F_2 + CH_4; IR fluorescence from HF	69
1b‴	$CH_3^\bullet$	6.6×10^{-12}	4.60	1.03×10^{-12}	300–400	thermal reactor-molecular beam; some fitting	70
1‴	$CH_3^\bullet$			1.2×10^{-12}	139–400	av of **1a‴**,**b‴**	
2‴	$CH_3CH_2^\bullet$			2.57×10^{-11}	298	$k_F/k_{O_2} + k_{O_2}$	71[d]
8a‴	$CF_3^\bullet$	4.4×10^{-12}	10.50	6.35×10^{-14}	256–342	review of competition experiments	72
8b‴	$CF_3^\bullet$			7.00×10^{-14}	295	thermal source; flow tube; MS detection	73
8c‴	$CF_3^\bullet$			1.50×10^{-14}	298	PLP of F_2 + CF_3H; IR fluorescence from HF	69
8‴	$CF_3^\bullet$			6.35×10^{-14}	256–342	use **8a‴**	
17‴	$CF_3CFH^\bullet$	1.27×10^{-12}	7.15	7.10×10^{-14}	298	$k_F/k_{O_2} + k_{O_2}$	23[e]

[a] $k_F = A \exp(-E/RT)$. Entries with only $k_{1,298}$ report no other temperature data. For cases with multiple reports, each is indicated by a numeral and letter designation while the selected data (see text) is indicated by the numeral only. The numerals correspond to those in Table 1. [b] A and $k_{F,298}$ in cm^3 molecule^{-1} s^{-1}, E in kJ/mol, and T in K. [c] See text for details. [d] $k_F/k_{O_2} = 3.3$; $k_{O_2} = 7.8 \times 10^{-12}$.[40] [e] $k_F/k_{O_2} = 0.6 \exp(-7.15/RT)$; $k_{O_2} = 2.12 \times 10^{-12}$.[24]

These were deconvoluted by a computer fit of the data to give the quite similar value **1b‴**. We use the average **1‴**.

The only value for ethyl (**2‴**) can be derived by combining a k_F/k_{O_2} ratio from a competition experiment, in which the kinetics of the reaction of very dilute F_2 with ethane with O_2 added were followed by the (small) rise in temperature in a static reactor at 298 K,[71] with the generally accepted value of k_{O_2}.[40] Value **8a‴** from a review[72] of data for trifluoromethyl is taken as **8‴**. It is consistent with **8b‴** derived from a flow reactor at 295 K with an upstream thermal source and real-time downstream MS detection.[73] Use of the IR emission from HF[69] gave a significantly lower value (**8c‴**), but the experiment was noted by the authors as much less sensitive than that for methyl (see above). Finally, k_F/k_{O_2} ratios were obtained by Kaiser[23] for 1,2,2,2-tetrafluoroethyl, 1,1-difluoroethyl, and 2,2-difluoroethyl but only for the first is a value of k_{O_2} available[24] that allows calculation of a value for **17‴**.

Computational Input. Curvature in Arrhenius plots for hydrogen transfer reactions is typically diagnostic of quantum mechanical tunneling which increasingly supplements the normal passage over the transition state (TS) barrier as T decreases. However, tunneling of an atom as heavy as chlorine seems less likely (but cf. ref 10). The extreme of negative Arrhenius energies is typically associated with a long-range attraction between the reactants and the barrierless formation of a weakly bound prereaction complex that precedes the TS, which itself may lie lower in energy than the separated reactants.[74] Over the past 15 years, the prototype $CH_3^\bullet + Cl_2$ reaction has been subjected to ab initio and TS theory computations at increasing levels of sophistication,[10,19,75−77] which we summarize in reverse chronological order.

Recent spin-unrestricted QCISD/6-311G(d,p) computations by Eskola and co-workers[10] identified a prereaction complex and a TS, both with a collinear C−Cl−Cl geometry (C_{3v} symmetry) (a weak postreaction complex was also found but does not influence the kinetics). In the prereaction complex, d_{C-Cl} was 1.77 times longer than in the final CH_3−Cl product, d_{Cl-Cl} was only 1.003 times longer than in Cl_2, and θ_{H-C-Cl} was 91.8° in comparison with the planar $CH_3^\bullet$ radical. In the continued movement to the TS along a linear coordinate, d_{C-Cl} decreased further to 1.37 times its final value, d_{Cl-Cl} increased only slightly to 1.05 times its original value, and θ_{H-C-Cl} expanded further to 97.2° compared with 108.8° in the final product. Coupled cluster theory at the complete basis set limit, including ZPE, gave the following relative enthalpies at 0 K: $CH_3^\bullet + Cl_2$, 0; prereaction complex, −4.5 kJ/mol; TS, +2.5 kJ/mol; $CH_3Cl + Cl^\bullet$, −108.8 kJ/mol (in good agreement with an experimental value of −107.6 kJ/mol, see below). Within the context of assumed 1D Cl tunneling, matching the experimental rate constant data at high T (Figure S-1), where tunneling would be minimal, required reducing the barrier by 0.9 kJ/mol, "well within the *ab initio* uncertainty," while matching the low T minimum (Figure S-1) required significantly increasing the imaginary frequency of the TS. On the other hand, good rate constant agreement could also be reached by reducing the barrier by 2.5−3 kJ/mol within modified TS theory, used when the TS lies below the ground state, without the need to invoke tunneling. In summary, the authors concluded that "the curvatures of the Arrhenius plots alone are not sufficient to discriminate whether the negative temperature dependences are caused by negative energies of the transition states or by the enhanced tunneling." Note that the starting materials and the TS lie tantalizingly close to each other in enthalpy.

Earlier computational results of Drougas and co-workers[77] were similar, with the bond distances in the starting materials, the precomplex, the TS, and the product all being slightly shorter and the relative energies being 0, −3.6, +5.2, and −126.4 kJ/mol (the latter is too negative; see below). Their kinetic computations were limited to the 300−600 K range, for which they found a slightly positive E, consistent with higher T experimental data;[11] they did not explore lower temperatures where the minimum was later found[10] (Figure S-1).

Still earlier, Lee and co-workers[76] found bond distances intermediate between the two studies[10,77] just summarized. The relative enthalpies at 298 K were method dependent. One gave values for the starting materials, precomplex, and TS of 0, −6.4, and +10.0 kJ/mol, respectively, and a second gave 0, −6.1, and −11.4 kJ/mol, respectively; i.e., the TS lay below the precomplex. For the latter values, computed rate constants as a function of T indeed showed a minimum, but at too high a temperature in comparison with experimental data (Figure S-1), and the TS had to be adjusted upward by 9.6 kJ/mol to approach the high-T data.[11] These authors also presented changes in computed Mulliken atomic charges as the reaction proceeds. The starting neutral $CH_3^\bullet$ had a −0.34 charge on C balanced by a +0.11 charge on each H. There was minimal shifting of charge in forming the precomplex: −0.36 on C, +0.12 on each H, +0.02 on the interior Cl, and −0.04 on the terminal Cl. However, there was a larger shift in the TS to −0.35 on C, +0.16 on each H (net +0.13), +0.01 on the interior Cl, and −0.13 on the terminal Cl. This trend continues

dx.doi.org/10.1021/jo2023075 | J. Org. Chem. 2012, 77, 2619−2636

to the product CH_3Cl, which had −0.26 on C, +0.14 on H (net +0.16), and −0.16 on Cl. These values are consistent with a TS contributor of the form $^{\delta+}CH_3\text{- - -}Cl\text{- - -}Cl^{\delta-}$ (see discussion of polar effects below).

Seetula[19] considered a broader range of larger alkylated and halogenated radicals at a more modest level of theory and concluded that the TS's for the fastest reactions had the longest d_{C-Cl} and the shortest d_{Cl-Cl}; in other words, as is common, the TS was most reactant-like for the fastest reactions. This was taken as evidence for an early loose TS for the very reactive ethyl with a gradual tightening toward the least reactive trichloromethyl. He noted that "for a loose TS a van der Waals interaction could be the main force attracting the two reactants." Tunneling was not considered important for the heavy Cl, and the curvature in Arrhenius plots was assigned to T dependences of the partition functions that determine A. Neither this computational study nor an even earlier one[75] identified a precomplex, although the latter authors suggested that the rate-determining step for the fastest reactions which showed a negative E might be the formation of such a species.

The highest level ab initio computations of which we are aware for the analogous $CH_3^\bullet + Br_2$ reaction[78] gave results very similar to those for the chlorine transfer. A collinear prereaction complex, TS, and postreaction complex were all identified. In the prereaction complex, d_{C-Br} was 1.60 times that in the final CH_3Br product, d_{Br-Br} was only 1.003 times that in Br_2, and θ_{H-C-Br} was 93.0°. In the continued movement to the TS, d_{C-Br} decreased further to 1.28 times its final value while d_{Br-Br} increased much less to only 1.02 times its original value; θ_{H-C-Br} expanded further to 97.9° in comparison with 108.3° in the final product. The relative energies were as follows: $CH_3^\bullet + Br_2$, 0; prereaction complex, −4.5 kJ/mol; TS, +1.0 kJ/mol; $CH_3Br + Br^\bullet$, −106.3 kJ/mol (in reasonable agreement with an experimental value of −100.2 kJ/mol, see below). RRKM and QCT calculations successfully reproduced the experimental value of $k_{Br,298}$ to within a factor of 1.5 as well as the slightly negative E. In summary, the authors concluded that "the slow decline in reactivity when increasing the initial reaction energy (i.e., temperature) [is an] expected consequence of the attractive character of the potential energy surface and the insignificant barrier at the entrance to the reaction."

Previous Attempted Structure−Reactivity Correlations of $k_X(R^\bullet)$. Empirical, semiempirical, and computational structure−reactivity relationships for the ubiquitous hydrogen transfer reaction $A^\bullet + H-B \rightarrow A-H + B^\bullet$ have received considerable attention, particularly to evaluate the relative importance of bond strength and polar effects (see ref 79 for a general review and ref 2 in ref 80 for a collection of specific methods). For example, we note the contrasting approaches of Roberts[81,82] and Zavitsas.[83−86] Roberts' empirical approach[81,82] to encompass wide variations in the structures of A and B in the exothermic direction considered several independent variables, including (a) the overall reaction enthalpy in terms of a modified form of the classic Evans−Polanyi relationship, $E = E_0 + \alpha\Delta_rH$, (b) the stabilization of the TS by polar effects ($^{\delta+}R\text{- - -}H\text{- - -}X^{\delta-}$) in terms of the square of the Mulliken electronegativity difference of $A^\bullet$ and $B^\bullet$, $[\chi_M(A) - \chi_M(B)]^2$, (c) the energy associated with structural changes of A and B between their radical state and the TS, such as pyramidalization of the radical center in going from the typically planar $A^\bullet$ toward the tetrahedral A−H, and (d) whether or not $B^\bullet$ was resonance-stabilized (not relevant to the present case of a departing halogen atom). One might hope that for the data in Tables 1−4 for halogen transfer (eq 2) which are limited to tricoordinate carbon-centered attacking radicals and a constant leaving radical, less complex formulations might suffice. Zavitsas' semiempirical approach[83−86] emphasized the repulsive interaction between A and B. Input parameters included the $D°$ values and the uncoupled vibrational frequencies of A−H, B−H, and A−B. An analogous treatment of eq 2 would require uncoupled IR frequencies for A−X, quantities not available for many of the rather complex A groups that will be considered.

Seetula and co-workers[18,19] categorized potential correlations of log $k_{Cl,298}$ with three independent variables: (a) the reaction enthalpy Δ_rH, (b) the difference between the ionization energy of $R^\bullet$ and the electron affinity of Cl_2, $IE(R^\bullet) - EA(Cl_2)$, and (c) the Thomas−Seetula electronegativity difference (TSED),[87,88] which defines a TSED parameter for a tricoordinate alkyl radical (i = 3) as the sum of the differences in Pauling electronegativity of each of the R′ substituents and that of H as a reference, i.e. $\Delta\chi = \sum_i[\chi_P(R'_i) - \chi_P(H)]$. Variable (a) provides in essence an Evans−Polanyi plot for $\Delta G^\ddagger$ rather than E (see below). Variables (b) and (c) represent different characterizations of a polar contribution to the TS. For the data then available, more limited than those in Table 1, the effectiveness of these approaches was judged to be (c) > (a) ≫ (b), and the authors focused on the TSED scale, especially "for reactions without barriers, which are essentially entropy-controlled, [for which] the TSED parameter...provides a good indicator of the importance of long-range interactions."

Earlier discussions by Gutman and his associates[22,39] had also focused on polar effects on the TS in the sense $^{\delta+}R\text{- - -}Cl\text{- - -}Cl^{\delta-}$, for which reaction should be facilitated by substituents on the radical center that stabilize a partially positive center, i.e., nucleophilic radicals, and they also promoted the TSED approach.[18] Unfortunately, the scope of this scale is limited because Pauling electronegativities were originally defined only for elements rather than functional groups. Seetula and co-workers expanded this range slightly by using an "effective" value of $\chi_P(Me) = 1.82$, which had been *fitted* for a previous correlation of the reaction $R^\bullet + HI$.[88] With this significant restriction, a quite good linear correlation of log $k_{Cl,300}$ indeed resulted for nine radicals which involved only H, Cl, Br, I, and Me as the substituents.[18] However, it deteriorated significantly for radicals containing F substituents (trifluoromethyl, difluorochloromethyl, and fluorodichloromethyl) which were "too fast". Their log $k_{Cl,300}$ values could be brought near the correlation line only by the unreasonably large change of $\chi_P(F)$ from 3.98 to 2.8.[20] A similarly good but limited correlation for $k_{Cl,500}$ was reported for a slightly different set of radicals with H, Cl, Br, and Me as the substituents.[19] In contrast, approach (b) failed badly[18,20] even when limited to the tricoordinate substituted methyl radicals; an attempt to include polarizabilities was not fruitful. However, Rissanen and co-workers[20] later portrayed a surprisingly good correlation between log $k_{Cl,298}$ and $EA(R^\bullet)$ (rather than $IE(R^\bullet)$), with decreasing reactivity associated with increasing electron affinity of the radical (see below). They proposed that "the formation of the bond between the radical center and Cl_2 in the reaction can be hindered by the higher the electron affinity of the radical... [because] the higher the electron affinity of the radical, the more the radical holds the electron and does not share it with Cl_2, which also has high EA."

Seetula and co-workers[18] also showed a plot of log $k_{Cl,300}$ vs Δ_rH_{298} for 16 reactions (largely a subset of Table 1): i.e., approach (a). If we remove the points for allyl and propargyl

dx.doi.org/10.1021/jo2023075 | J. Org. Chem. 2012, 77, 2619−2636

because of overly long T extrapolations and the points for the non-tricoordinate vinyl and formyl, the correlation appears promising (no statistical parameters were given) except for trifluoromethyl and difluorochloromethyl, which were now "too slow." These authors, however, gave less credence to the importance of an enthalpy effect than a polar effect. We note that there is some ambiguity in any Evans–Polanyi plots shown in the literature for eq 2 because of uncertainties in the values for $\Delta_r H_{298}$ (see below).

In contrast, Lee and co-workers[76] focused instead on the enthalpy effect and did not consider polar effects. They plotted 20 data points for chlorine transfer in standard Evans–Polanyi format and recommended $A = (3.90 \pm 5.10) \times 10^{-12}$ and $E = (0.38 \pm 0.04)\Delta_r H + (42.3 \pm 3.4)$. However, this correlation excluded isopropyl and *tert*-butyl (presumably because of negative E values), as well as vinyl, 1,2-dichloroethyl, and trifluoromethyl, the latter being much "too slow."

An attempted correlation of log $k_{Br,298}$ with the TSED independent variable (χ_P(Me) was again set by fitting as above) was quite successful for alkyl and halogen substituents[18] but, as for $k_{Cl,298}$, it performed badly for all the F-bearing radicals.

Considering the relative reactivity of the four halogens, Evans and Whittle[89] compared several values of k_{Cl} and k_{Br} and noted that $k_{Br}/k_{Cl} > 1$ even though bromine transfer is *less* exothermic and therefore concluded that "the important factor [in this competition] is not $\Delta_r H$ but the strength of the bond broken": i.e., $D°$(Cl–Cl) > $D°$(Br–Br). Timonen and co-workers[41,43,48] also noted that reactivity for comparative halogen transfer frequently runs counter to Evans–Polanyi expectations. For example, fluorine transfer forms much the strongest C–X bonds while breaking one of the weaker X–X bonds, yet it is at the low end of the kinetic spectrum. They therefore suggested that "reactivity correlates best with properties that reflect the magnitudes of long-range attractive forces, particularly those associated with the stabilization of intermediate states having some form of charge separation." This research group[41,43,48] suggested qualitatively that the increasing polarizability of the halogens from F_2 to I_2 should promote reactivity but did not present a specific correlation. Krech and McFadden[90] specifically proposed an inverse relationship between E for the generic $A^\bullet + B–C \rightarrow A–B + C^\bullet$ reaction and the mean polarizability, α, of the B–C molecule and noted that this correlation seemed particularly reliable for *halogen transfer*, although the database then available was small for cases where $A^\bullet$ was an organic radical. Their reasoning was that "Attractive dispersion forces lower the interaction energy as reactants approach to distances characteristic of the onset of reaction. These forces are proportional to polarizability among other factors; thus the greater the polarizabilities of the reactants, the less repulsive the approach." (We will discuss further below the overall reactivity order for the halogens, which is $I_2 > Br_2 \gg Cl_2 \approx F_2$.)

RESULTS AND DISCUSSION

Given the occurrence of curved Arrhenius plots, i.e., $E = f(T)$, and negative E values, as well as cases where the rate constant is reported only for 298 K, several authors who have explored correlations for eq 2 have used log k_{298}, i.e., $\Delta G^{\ddagger}_{298}$, rather than E as the dependent variable (cf. refs 12 and 18–20), and we also adopted this approach, remembering that this was the original intent of the Evans–Polanyi formalism.[91] If E (the empirical Arrhenius slope) is T dependent, then the Arrhenius formalism demands that A (the empirical intercept) also be T dependent and interpretations in the literature of comparative A values become suspect. Also note a significant oversimplification of our approach in that the most reactive cases may well involve an entropy-controlled barrierless process while the least reactive clearly have significantly positive E values.

General Reactivity Trends. Before exploring specific structure–reactivity relationships, we make some general observations concerning the often discussed polar effect arising from a $^{\delta+}$R- - -X- - -X$^{\delta-}$ contribution to the TS, ignoring for the moment any concurrent enthalpy effect. If this effect is significant, an electronegative substituent on the radical center which withdraws electrons by a σ inductive and/or field effect should destabilize the TS and thereby decrease $k_{X,298}$. However, it is well-known that electronegative substituents with lone electron pairs can also stabilize a positive center by π electron donation. Hence, we expect a competition between these deactivating and activating "effects", and we first show that this is a reasonable semiquantitative assumption.

We begin with the most voluminous data for chlorine transfer (Table 1). Consider the effects of α substituents in the $XCH_2^\bullet$ family. If we assign a *relative* log $k_{Cl,298}$ = 0.00 to the parent methyl (X = H, **1**), a methyl substituent (X = Me, **2**), is activating by 0.97 log unit while the halogens are deactivating by −0.75, −0.56, and −0.28 log units for X = Cl (**9**), Br (**12**), and I (**13**), respectively. This contrast between electron-donating and electron-withdrawing groups indeed conforms simplistically to an inductive/field polar effect on the polarized TS. However, this effect alone would be grossly inconsistent with the fact that oxygen functionality is activating by 1.24 log units for X = OH (**31**) and 1.58 log units for X = OMe (**32**); in fact, methoxymethyl is the most reactive radical in the data set. This would suggest an active role for π donation as well, which dominates for oxygen, while inductive/field withdrawal dominates for the halogens. The −0.81 log unit deactivating effect for X = SH (**29**) but 0.63 log unit activating effect for X = SMe (**30**) leaves the effect of sulfur ambiguous (and the kinetic data for these cases questionable). The carbonyl group, X = EtC(=O) (**33**), is very deactivating by −1.79 log units; this also supports development of partial positive charge at the radical center. Finally, the phenyl group (X = Ph, **6**) has little effect, only −0.11 log units deactivating.

The series methyl (**1**), ethyl (**2**), isopropyl (**6**), and *tert*-butyl (**7**) gives values on the relative log scale of 0.00, 0.97, 1.54, and 1.39 (Figure S-3). Hence the cumulative effect of activating methyl substituents appears to saturate. A similar trend can be seen in the data for *n*-butyl (**4**), *sec*-butyl (**5**), and *tert*-butyl (**7**), whose relative values on the log scale are 1.13, 1.46, and 1.39. The accumulation of deactivating chloro substituents in the series methyl (**1**), chloromethyl (**9**), dichloromethyl (**10**), and trichloromethyl (**11**) gives relative values on the log scale of 0.00, −0.75, −1.99, and −3.93 (Figure S-4). Hence for both series, the size of the substituent effect decreases as the absolute reactivity increases, i.e., as E decreases, but not in a purely additive fashion. Combining a methyl (0.97 log unit activating) and a chloro substituent (−0.75 log unit deactivating) in 1-chloroethyl (**27**) leads to a relative log value of 0.28, in comparison with the arithmetic sum of 0.22. Adding a second chloro substituent in 1,1-dichloroethyl (**33**) leads to a relative log value of −1.14, compared with the arithmetic sum of −0.53. Both the TSED scale (see above) and the Hammett scales that we will introduce below use an arithmetic sum of parameters for the three substituents. However, these examples of moderately nonadditive substituent effects indicate that such

dx.doi.org/10.1021/jo2023075 | J. Org. Chem. 2012, 77, 2619–2636

approaches have inherent limitations that should be recognized upfront. We will explore the use of a nonlinear function below.

Compare next the effects of β substituents, for which exercise we set the *relative* log $k_{Cl,298}$ = 0.00 for ethyl (rather than for methyl as above). Not surprisingly, the reactivities of 1-propyl (**3**) and 1-butyl (**4**) are only slightly greater than those of ethyl by 0.09 and 0.16 log unit. However, 2-chloroethyl (**24**) is deactivated by −1.30 log units and is in fact 0.61 log unit *less* reactive than the 1-chloro isomer (**27**). Such a directionality is unlikely for a purely inductive/field effect that falls off with distance and suggests that the TS for 1-chloroethyl receives some stabilization from π-donation from chlorine that partially offsets its dominant electron-withdrawing properties.

Finally, although the most electronegative substituent in Table 1 is F, trifluoromethyl is notably *more* reactive than trichloromethyl. For the series trichloromethyl (**11**), fluorodichloromethyl (**14**), difluorochloromethyl (**15**), and trifluoromethyl (**8**), the *relative* $k_{Cl,298}$ values on a log scale are 0.00, 1.40, 2.42, and 2.25, respectively. Thus, while the series is again not monotonic, generally an α-F substituent is considerably *less* deactivating than an α-Cl substituent. This order conforms to the usual observation that π-donation by F is more effective than that by Cl.

For $k_{Br,298}$ (Table 2), the activating effect of a methyl substituent again appears to saturate, the *relative* values for methyl (**1′**), ethyl (**2′**), isopropyl (**6′**) and *tert*-butyl (**7′**) being 0.00, 0.40, 0.55, and 0.39 on a log scale. The accumulation of deactivating chloro substituents in the series methyl (**1′**), chloromethyl (**9′**), dichloromethyl (**10′**), and trichloromethyl (**11′**) gives *relative* values on a log scale of 0.00, −0.45, −1.35, and −3.19. Hence, as for chlorine transfer, the cumulative substituent effects are not strictly additive but become more compressed as the reactivity increases: i.e., as E decreases. For the series trichloromethyl (**11′**), fluorodichloromethyl (**14′**), difluorochloromethyl (**15′**), and trifluoromethyl (**8′**), the *relative* values on a log scale are 0.00, 1.45, 1.78, and 1.72, respectively. Hence, again as for chlorine transfer, an α-F substituent is generally *less* deactivating than an α-Cl substituent.

Single-Variable Correlations of $k_{X,298}$ for X = Cl, Br: The Enthalpy Effect. We begin our exploration with the three potential independent variables considered by Seetula,[18,19] applied to the expanded and modified data sets in Tables 1 and 2. The values of the updated independent variables used are compiled in Table S-1. The regression equations and correlation indicators, especially the mean unsigned deviation (MUD) in log units, where the "deviation" is log k_{calcd} − log k_{exp}, are compiled in Tables 5−7.

To maintain historical perspective, the Evans−Polanyi formulation takes precedence. (Strictly speaking, the classic Evans−Polanyi equation has normally been used to correlate the reactivity of a single radical with a series of hydrogen transfer agents in the exothermic direction, while the present case involves the reaction of a series of radicals with a single halogen transfer agent in the exothermic direction.) For step 2, Δ_rH_{298} = $D°$(X−X) − $D°$(R−X). The required $D°$(R−X) values were taken from the recent compilation by Luo,[92] although there are modest disagreements in the literature for several of them. We consider only X = Cl and Br because the data for X = F and I are much too limited to warrant regression.

For $k_{Cl,298}$, values of Δ_rH_{298} are available for 24 of the 36 entries in Table 1. The least-squares regression is shown as **A** in Table 5 and Figure 1. Although there is the expected trend for the more exothermic cases to be more rapid, the quantitative correlation is poor with MUD > 1 log unit, i.e., the highly exothermic chlorine transfer reaction does not correlate well with reaction enthalpy, as already noted.[18] As a dramatic example, Δ_rH_{298} for the least exothermic cases trichloromethyl (**11**) and benzyl (**36**) differs by only 3.3 kJ/mol but the latter is almost 4 orders of magnitude more reactive. As an inverse example, Δ_rH_{298} for trifluoromethyl (**8**) and 2-oxo-1-butyl (**33**) differs by 56 kJ/mol but their reactivities are virtually identical.

For a parallel treatment of a smaller number (n = 13) of $k_{Br,298}$ values in Table 2, the correlation (**A′** in Table 6) was again poor. As a dramatic example, Δ_rH_{298} for the least exothermic cases trichloromethyl (**11′**) and allyl (**37′**) differs by only 5.8 kJ/mol but the latter is $2^1/_2$ orders of magnitude more

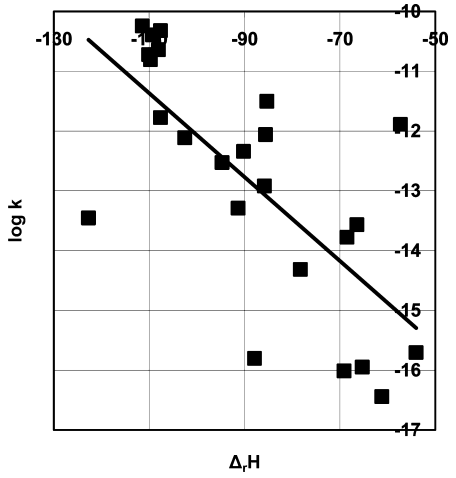

Figure 1. Dependence of log $k_{Cl,298}$ (cm^3 molecule^{-1} s^{-1}) on Δ_rH_{298} (kJ/mol) (A in Table 5).

Table 5. Regression Equations for Various Correlations of log $k_{Cl,298}$

correlation	log $k_{Cl,298}$[a]	n[b]	MUD[c]	r^2[d]
A	(−19.08 ± 1.37) − (0.0701 ± 0.0151) (Δ_rH_{298})[e]	24	1.09	0.50
B	(−11.54 ± 0.40) − (0.592 ± 0.207) (TSED)[f]	25	1.09	0.27
C	(−11.91 ± 0.37) − (0.208 ± 0.061) (TSED*)[g]	27	1.16	0.32
D	(−6.46 ± 2.20) − (0.979 ± 0.390) (IE(R•) − EA(Cl_2))[h]	20	1.03	0.26
E	(−10.81 ± 018) − (1.701 ± 0.147) (EA(R•))[i]	23	0.43	0.86
F	(−15.86 ± 0.55) + (0.238 ± 0.033) ((χ_M(R•) − χ_M(Cl•))^2)	19	0.55	0.75
G	(−11.75 ± 0.10) − (4.735 ± 0.221) ($\sum\sigma_p$)	36	0.42	0.931
H	(−11.66 ± 0.11) − (4.264 ± 0.319) ($\sum\sigma_p$) − (0.993 ± 0.5025) ($\sum\sigma_p$)^2	36	0.38	0.939
G*[j]	(−11.86 ± 0.11) − (4.517 ± 0.320) ($\sum\sigma_p$)	17	0.30	0.930
H*[j]	(−11.33 ± 0.06) − (3.930 ± 0.156) ($\sum\sigma_p$) − (3.340 ± 0.416) (($\sum\sigma_p$)^2)	17	0.14	0.988
I	(−11.12 ± 0.21) − (3.826 ± 0.326) ($\sum\sigma_m$)	36	0.65	0.80
J	(−12.75 ± 0.17) − (3.371 ± 0.387) ($\sum\sigma_p^+$)	28	0.70	0.75
K	(−11.54 ± 0.14) − (4.742 ± 0.208) ($\sum\sigma_I$) − (4.130 ± 0.348) ($\sum\sigma_R$)	36	0.39	0.940

[a] k in cm^3 molecule^{-1} s^{-1}. [b] Number of cases from Table 1 for which the required independent variable(s) were available. [c] Mean unsigned deviation of log k_{exp} from log k_{calcd}. [d] Correlation coefficient of least-squares regression. [e] Δ_rH_{298} in kJ/mol. [f] Includes TSED parameters for groups as well as atoms; see text and ref 86. [g] TSED* preserves the TSED format but uses Mulliken rather than Pauling electronegativities. [h] IE(R•) in eV; EA(Cl_2) = 2.4 eV. [i] EA(R•) in eV. [j] Truncated set limited to alkyl and halogen substituents; see text.

dx.doi.org/10.1021/jo2023075 | J. Org. Chem. 2012, 77, 2619−2636

Table 6. Regression Equations for Various Correlations of $k_{Br,298}$

correlation	log $k_{Br,298}$ [a]	n [b]	MUD [c]	r^2 [d]
A′	(−13.71 ± 1.14) − (0.0304 ± 0.0133) (Δ_rH_{298}) [e]	13	0.81	0.32
B′	(−10.51 ± 0.32) − (0.397 ± 0.137) (TSED) [f]	14	0.59	0.41
C′	(−11.40 ± 0.23) − (0.129 ± 0.040) (TSED*) [g]	14	0.59	0.47
D′	(−8.12 ± 1.80) − (0.519 ± 0.289) (IE(R•) − EA(Br_2)) [h]	16	0.73	0.19
E′	(−10.22 ± 0.21) − (1.051 ± 0.161) (EA(R•)) [i]	15	0.35	0.77
G′	(−10.77 ± 0.15) − (2.668 ± 0.377) ($\sum\sigma_p$)	16	0.40	0.78
H′	(−10.61 ± 0.17) − (2.253 ± 0.436) ($\sum\sigma_p$) − (1.549 ± 0.942) (($\sum\sigma_p$)^2)	16	0.38	0.82
I′	(−10.39 ± 0.20) − (1.806 ± 0.274) ($\sum\sigma_m$)	16	0.378	0.76
J′	(−11.32 ± 0.22) − (1.860 ± 0.622) ($\sum\sigma_p^+$)	15	0.70	0.41
K′	(−10.54 ± 0.21) − (2.469 ± 0.382) ($\sum\sigma_I$) − (1.859 ± 0.636) ($\sum\sigma_R$)	16	0.36	0.81

[a] k in cm^3 molecule^{-1} s^{-1}. [b] Number of cases from Table 2 for which the required independent variable(s) were available. [c] Mean unsigned deviation of log k_{exp} from log k_{calcd}. [d] Correlation coefficient of least-squares regression. [e] Δ_rH_{298} in kJ/mol. [f] Includes TSED parameters for groups as well as atoms; see text and ref 86. [g] TSED* preserves the TSED format but uses Mulliken rather than Pauling electronegativities. [h] IE(R•) in eV; EA(Br_2) = 2.42 eV. [i] EA(R•) in eV.

Table 7. Regression Equations for Dual-Variable Correlations of log $k_{Cl,298}$

	log $k_{Cl,298}$ [a]	n [b]	MUD [c]	r^2 [d]
G [e]	(−11.75 ± 0.10) − (4.735 ± 0.221) ($\sum\sigma_p$)	36	0.42	0.931
Gabr [f]	(−11.75 ± 0.12) − (4.782 ± 0.253) ($\sum\sigma_p$)	24	0.388	0.942
Gaug [g]	(−11.41 ± 0.77) − (4.912 ± 0.385) ($\sum\sigma_p$) + (0.00354 ± 0.00778) (Δ_rH)	24	0.392	0.943
E [e]	(−10.81 ± 018) − (1.701 ± 0.147) (EA(R•))	23	0.43	0.86
Eabr [f]	(−10.90 ± 0.15) − (1.632 ± 0.148) (EA(R•))	18	0.40	0.88
Eaug [g]	(−11.71 ± 0.87) − (1.522 ± 0.189) (EA(R•)) − (0.00785 ± 0.00827) (Δ_rH)	18	0.37	0.89
F [e]	(−15.86 ± 0.55) + (0.238 ± 0.033) ((χ_M(R•) − χ_M(Cl•))^2)	19	0.55	0.75
Fabr [f]	(−15.87 ± 0.61) + (0.243 ± 0.039) ((χ_M(R•) − χ_M(Cl•))^2)	16	0.58	0.74
Faug [g]	(−17.69 ± 0.80) + (0.200 ± 0.035) ((χ_M(R•) − χ_M(Cl•))^2) − (0.0268 ± 0.0093) (Δ_rH)	16	0.48	0.84

[a] k in cm^3 molecule^{-1} s^{-1}. [b] Number of cases from Table 1 for which the required independent variable(s) were available. [c] Mean unsigned deviation of log k_{exp} from log k_{calcd}. [d] Correlation coefficient of least-squares regression. [e] From Table 5. [f] Abridged by lower value of n because of limited availability of Δ_rH values. [g] Augmented by addition of a term in Δ_rH.

reactive. As an inverse example, Δ_rH_{298} for trifluoromethyl (**8′**) and difluorochloromethyl (**15′**) differs by 26 kJ/mol but their reactivities are virtually identical.

Single-Variable Correlations of $k_{X,298}$ for X = Cl, Br: The Polar Effect. *TSED.* We consider the two possible descriptors of the polar effect suggested by Seetula,[18] i.e., the TSED parameter and the quantity IE(R•) − EA(Cl_2), along with the quantity [χ_M(R•) − χ_M(Cl•)]^2 adapted from the Roberts[81] treatment of hydrogen transfer, where χ_M is the Mulliken electronegativity defined as [IE(A) + EA(A)]/2, the unusual parameter EA(R•) considered by Rissanen and workers,[20] and a new approach based on Hammett substituent constants. As already noted,[22,39] the TSED parameter based on the classic Pauling electronegativity values[93] for the R′ substituents gave an excellent correlation for our data set (Figure 2, upper portion) (n = 12, MUD = 0.26 log unit, and r^2 = 0.95) if limited to R′ = H, Cl, Br, I, Me, with χ_P(Me) assigned as 1.82. However, if properly extended to include the three F-substituted radicals, the correlation indicators were significantly degraded (n = 15, MUD = 0.72 log unit, and r^2 = 0.61), even given the somewhat arbitrary assignment of χ_P(Me). The number of cases included can be almost doubled (n = 25) by retaining the TSED formalism but using the χ_P values for groups as well as atoms (Table S-1) as derived by Zavitsas[86] from substituting known $D°$ values into the Pauling equation $D°$(A–B) = $^1/_2$[$D°$(A–A) + $D°$(B–B)] + 96.5[χ_P(A) − χ_P(B)]^2 anchored to χ_P(OH) = 3.50; this involves a major increase in χ_P(Me) from the assigned 1.82 to 2.53, which shifts several data points to the right. However, the TSED correlation with these parameters (Figure 2, lower portion; **B** in Table 5) is significantly degraded with MUD > 1 log unit. In a second attempt to broaden the range of applicability of the TSED approach, we retained its formal definition but substituted χ_M for χ_P, values of which are also available[81,94] for several groups as well as atoms; we also changed χ_M(H) from 7.17 to 5.05, as recommended by Roberts.[81] This modification, labeled TSED* (**C** in Table 5; plot not shown), offered no improvement over the first attempt. Thus, the TSED parameter is not promising for application to the wider range of data in Table 1.

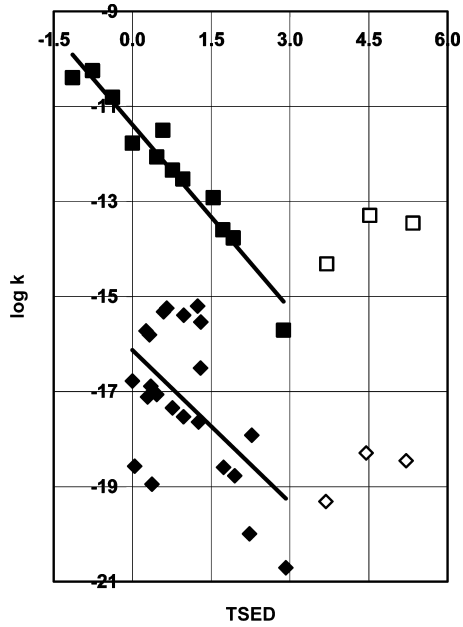

Figure 2. Dependence of log $k_{Cl,298}$ (cm^3 molecule^{-1} s^{-1}) on TSED: (upper set) traditional χ_P values, with solid squares denoting all alkyl and halogen substituents except F and open squares denoting F substituents; (lower set) offset by −5 log units, with χ_P values from ref 86 and solid diamonds denoting all substituents except F and open diamonds denoting F substituents.

For $k_{Br,298}$, correlation **B′** in Table 6 includes values for the three F-containing radicals and is based on the χ_P values of Zavitsas.[86] Correlation **C′** uses the TSED* modification as defined above. While both performed somewhat better than for the corresponding treatments of $k_{Cl,298}$ in Table 5 (albeit for only about half the number of cases with less structural diversity), the correlation indicators remained modest.

[IE(R•) − EA(Cl_2)]. The regression with the parameter IE(R•)[95] − EA(Cl_2) for 20 of the cases of $k_{Cl,298}$ in Table 1 is shown in Figure 3

dx.doi.org/10.1021/jo2023075 | J. Org. Chem. 2012, 77, 2619–2636

and **D** in Table 5. Although there is uncertainty in some of the IE(R•) values, MUD remained >1 log unit. A parallel treatment of log $k_{Br,298}$ (**D′** in Table 6) also gave no improvement over the correlations with TSED or TSED*.

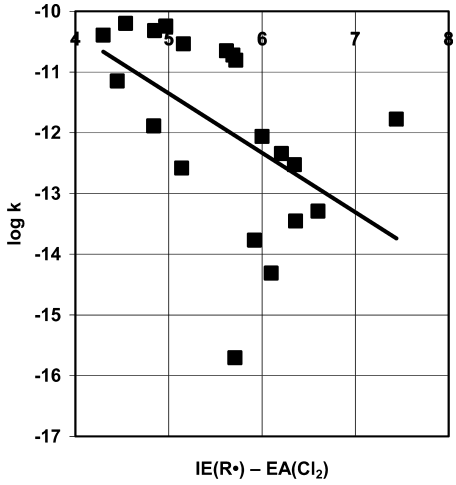

Figure 3. Dependence of log $k_{Cl,298}$ (cm^3 $molecule^{-1}$ s^{-1}) on IE(R•) – EA(Cl_2) (**D** in Table 5).

$[\chi_M(R^\bullet) - \chi_M(Cl^\bullet)]^2$. Following the lead of Roberts[81] used for hydrogen transfer, we performed a regression of log $k_{Cl,298}$ with $\Delta\chi_{AB}{}^2 = [\chi_M(R^\bullet) - \chi_M(Cl^\bullet)]^2$; note the use here of $\chi_M(R)$, not $\chi_M(R')$. As seen in Figure 4 and **F** in Table 5, the degree of correlation was much improved over that with TSED, TSED*, or IE(R•) – EA(Cl_2),[20] although it remained slightly poorer than the surprising result with EA(R•) to be addressed next.

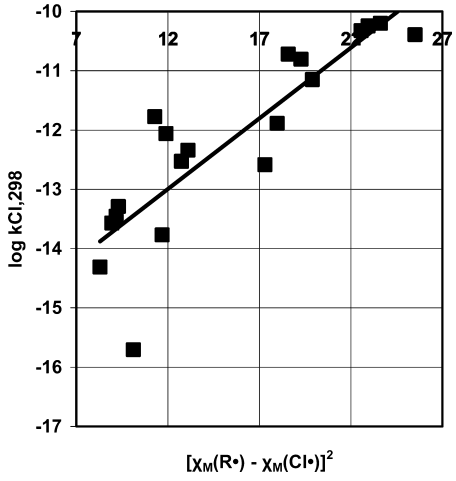

Figure 4. Dependence of log $k_{Cl,298}$ on $[\chi_M(R^\bullet) - \chi_M(Cl^\bullet)]^2$ (**F** in Table 5).

EA(R•). We also repeated the recent correlation with EA(R•) used by Rissanen and co-workers,[20] values being available[20,95] for 23 of the cases of $k_{Cl,298}$ in Table 1. Although this seems like an unusual independent variable to treat the generally accepted polarization direction $^{\delta+}$R- - -Cl- - -Cl$^{\delta-}$ which is supported by high-level computations,[76] the result shown in Figure 5 and **E** in Table 5 was surprisingly good, very much better than that with IE(R•) – EA(Cl_2).[20] The reactivity rather smoothly decreases as EA(R•) increases. Such a dependence is reminiscent

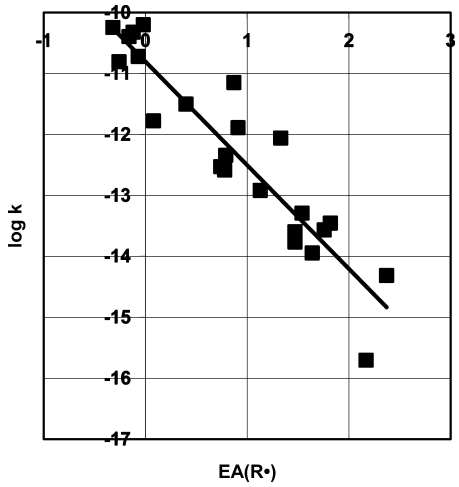

Figure 5. Dependence of log $k_{Cl,298}$ on EA(R•) (eV) (**E** in Table 5).

of an empirical postulate by Alfassi and Benson[97] that the TS for generic atom transfer can be pictured as having two one-electron bonds, A·B·C, with a third antibonding electron shared between the terminal groups A and C, and that therefore *E* should be dependent on properties of A and C but relatively unaffected by the nature of B. One of the resulting correlations suggested was in fact: $E = a - b[EA(A) + EA(C)]$, i.e. increasing electron affinity of *either* A or C would stabilize the antibonding electron and decrease *E*. However, in our case, the sign of the slope is "wrong"; i.e, as EA(R•) increases, $k_{Cl,298}$ *decreases* rather than increases. Therefore, this seems an opportune time to remind ourselves of the axiom that correlation does not necessarily indicate causation. We have already seen, and will see more clearly below, that reactivity for chlorine transfer generally decreases as the substituents on the radical move from stabilizing to destabilizing a positive center (and inversely from destabilizing to stabilizing a negative center). This is indeed the direction that will increase IE(R•) but, given the "opposite" sign conventions of IE(R•) and EA(R•), will also increase EA(R•). It is not clear however why the correlation with EA(R•) should be notably better than with IE(R•). The same counterintuitive result occurred for bromine transfer (**E′** in Table 6).

Hammett Parameters. As a possible alternative to representing the polar effect at the radical center with χ, IE, or EA values, we explored use of the venerable and widely available Hammett substituent constants.[96] Specifically we were attracted to σ_p because it is known to include both the σ inductive/field and π-resonance electron-donating or -withdrawing capabilities of a substituent. In fact, σ_p can be decomposed into the sum of σ_I (or *F*) and σ_R (or *R*).[96] We define $\sum\sigma_p$ as the sum of the σ_p constants for the three R′ groups. The linear least-squares regression for $k_{Cl,298}$, for which $\sum\sigma_p$ is available for *all* 36 entries, is shown as eq 3, as **G** in Table 5, and as the solid line in the upper portion of Figure 6. Especially given the much wider structural range of R′ treated than in the earlier entries in Table 5, the quality of this correlation is the best so far. However, with a modicum of imagination, one might detect curvature in the data in Figure 6. Therefore, as an arbitrary approach to allow curvature, we carried out a parallel regression with the less conventional quadratic equation shown as H in Table 5 and as the dashed line in the upper portion of Figure 6, but the correlation parameters were only marginally improved. To the extent that the quadratic formulation has any physical meaning,

dx.doi.org/10.1021/jo2023075 | J. Org. Chem. 2012, 77, 2619–2636

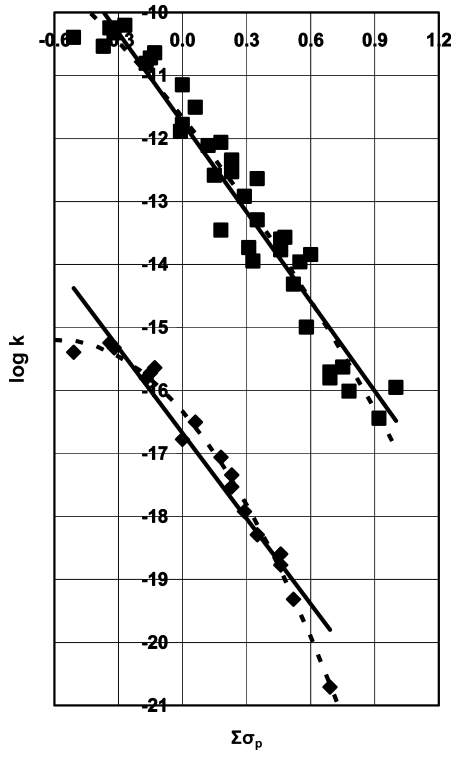

Figure 6. Dependence of log $k_{Cl,298}$ (cm^3 $molecule^{-1}$ s^{-1}) on $\sum\sigma_p$: (upper portion) solid line gives the linear correlation (**G** in Table 5) and the dashed line the quadratic correlation (**H** in Table 5) for all 36 data points; (lower portion) solid line gives the linear correlation (**G*** in Table 5) and the dashed line the quadratic correlation (**H*** in Table 5) for a truncated set of 17 data points (see text). log *k* in the lower portion is offset by −5 log units.

$k_{Cl,298}$ may be approaching asymptotically a structurally insensitive, encounter-controlled upper limit for the most reactive cases (most electron-donating substituents and negative $\sum\sigma_p$) while it is becoming gradually more sensitive to substituent effects on a polar TS as reactivity decreases (most electron-withdrawing substituents and positive $\sum\sigma_p$ values), as suggested by Figures S-3−S-5. Indeed when we chose a subset of the data consisting of all the cases with only alkyl and halogen substituents on the radical center (**1**−**7**, **9**−**16**, and **27** and **28**), except for trifluoromethyl, the quadratic plot showed more curvature, as shown in the lower portion of Figure 6, and gave an excellent fit with a MUD of only 0.14 log unit and $r^2 = 0.988$. Thus, it is especially the "slow" cases of trifluoromethyl (**8**), 2-butanon-3-yl (**34**), and 3-pentanon-2-yl (**35**) that are reducing the curvature in the upper portion of Figure 6.

$$\log k_{Cl,298} = (-11.75 \pm 0.10) - (4.735 \pm 0.221)(\sum \sigma_p) \quad (3)$$

In contrast to the original limited TSED scale, the fluorinated cases, fluorodichloromethyl (**14**) and difluorochloromethyl (**15**), fall very close to either Hammett correlation line, although trifluoromethyl (**8**) is "too slow". This significant improvement results because $\sigma_p(F) = 0.06$ is less positive, i.e., less electron withdrawing, than $\sigma_p(Cl) = 0.23$, in contrast to the greater $\chi(F)$. Using the dissection $\sigma_p = \sigma_I + \sigma_R$, we have $\sigma_p(F) = \sigma_I(F) + \sigma_R(F) = 0.45 - 0.39 = 0.06$ and $\sigma_p(Cl) = \sigma_I(Cl) + \sigma_R(Cl) = 0.42 - 0.19 = 0.23$. In other words, the inductive/field electron-withdrawing contribution is indeed slightly greater for fluorine than for chlorine but this is more than offset by its significantly greater π-electron-donating contribution. This rationalizes the generally lesser deactivation of halogen transfer by an added F substituent than a Cl substituent noted above. The extremes of this trend in the data set are represented by R′ = OH, for which $\sigma_p(OH) = \sigma_I(OH) + \sigma_R(OH) = 0.33 - 0.70 = -0.37$, and R′ = OCH_3, for which $\sigma_p(OMe) = \sigma_I(OMe) + \sigma_R(OMe) = 0.29 - 0.56 = -0.27$. In both cases π donation is greater than σ-withdrawal, σ_p becomes negative, and the hydroxymethyl (**31**) and methoxymethyl (**32**) radicals are more reactive than even ethyl (**2**). (This high reactivity of methoxymethyl compared with alkyl radicals was noted without rationalization by Sehested.[33])

The good correlation in Figure 6 suggests that the classic σ_p parameter, which represents an empirical balance of σ-withdrawing and π-donating properties, is an appropriate variable to characterize the chlorine transfer reaction. Hence, it is not surprising that regressions with the σ_m parameter, which has minimal input from resonance effects, and with the σ_p^+ parameter, which highlights resonance with strongly electron-demanding reaction centers, were both less effective than the use of σ_p as shown in **I** and **J** in Table 5. As additional confirmation of this conclusion, a regression was carried out in which the σ_I and σ_R components of σ_p were decoupled and both were allowed to be independent variables. The result is shown as **K** in Table 5 and is almost indistinguishable from **G** and **H** that used $\sum\sigma_p$ alone, with the coefficients of $\sum\sigma_I$ and $\sum\sigma_R$ being almost equal.

The corresponding linear and quadratic regressions for $k_{Br,298}$ with $\sum\sigma_p$, shown as **G′** and **H′** in Table 6 and as Figure 7, do not have correlation parameters quite as good as those for chlorine transfer (Figure 6), but the selection of radical substituents is not as broad (only about half the number of cases). Again the quality of the quadratic fit is only marginally improved over the simple linear fit. As for chlorine transfer and in contrast to the TSED scale, the fluorinated cases are not notable outliers. For the smaller range of substituents for bromine transfer, the difference between the correlations with $\sum\sigma_m$ (**I′**) and $\sum\sigma_p$ (**G′**) was significantly less, while the difference between $\sum\sigma_p^+$ (**J′**) and $\sum\sigma_p$ (**G′**) was greater. A regression with the σ_I and σ_R components of σ_p decoupled (**K′** in Table 6) showed a somewhat larger coefficient for $\sum\sigma_I$ than for $\sum\sigma_R$, whereas for chlorine transfer they were virtually equal. Hence, although again the set of substituents is different, there thus may be a hint that bromine transfer is relatively more susceptible than is chlorine transfer to the inductive/field effect compared with the resonance effect.

Dual-Variable Correlations of $k_{X,298}$ for X = Cl. *Indicators of the Polar Effect and Δ_rH.* The historical approach to treat a combined enthalpy of reaction effect and a polar effect has been to use a separate variable for each. Therefore, we amended the best three predictors found above for the polar effect on $k_{Cl,298}$ by adding a term in Δ_rH. In each case the value of *n* was somewhat reduced by the availability of Δ_rH values. The resulting correlations are summarized in Table 7 for the original single-variable correlation (see Table 5), the slightly abridged single-variable correlation for the necessarily reduced *n*, and the augmented dual-variable correlation with Δ_rH added. The (small) improvement in MUD from the added term was greatest for the correlation with $[\chi_M(R^\bullet) - \chi_M(Cl^\bullet)]^2$, which had been the least successful of these three parameters on its own. On the other hand, the change in MUD from the added term was insignificant for the correlation with $\sum\sigma_p$, which had been the most successful on its own, and in fact the Δ_rH term has a

dx.doi.org/10.1021/jo2023075 | J. Org. Chem. 2012, 77, 2619−2636

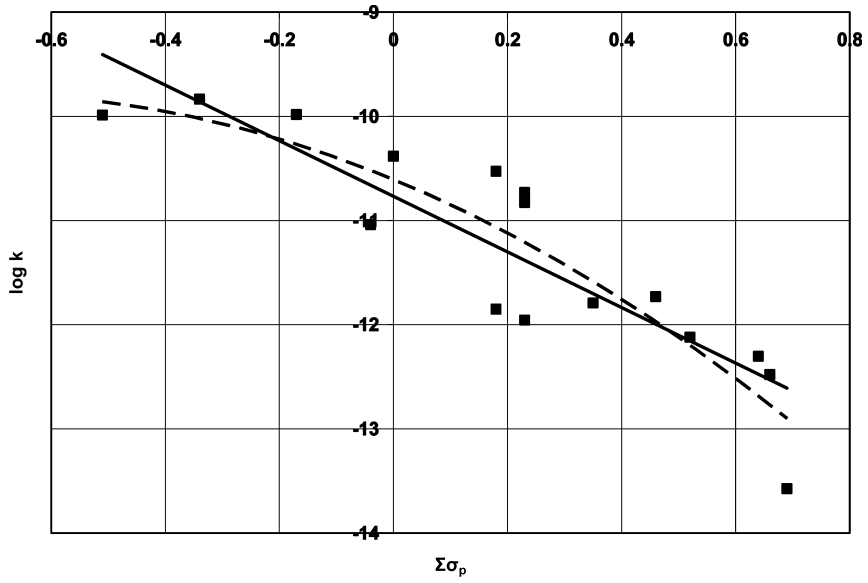

Figure 7. Dependence of log $k_{Br,298}$ (cm^3 molecule^{-1} s^{-1}) on $\sum\sigma_p$: (solid line) linear correlation (**J′** in Table 6); (dashed line) quadratic correlation (**K′** in Table 6).

very small *positive* coefficient which corresponds to a "contra-Evans-Polanyi" contribution.

$\sum\sigma_p$ Indicator of the Polar Effect and the Degree of Substitution at the Radical Center. One might consider whether increasing steric congestion between the approaching radical and the halogen molecule as the radical center becomes more highly substituted with non-H substituents would retard the halogen transfer reaction. Note that for our definition of "deviation" (see above), a positive deviation indicates that the observed rate constant is less ("too slow") than that predicted by the particular correlation, and vice versa. If we focus on the correlation of log $k_{Cl,298}$ with $\sum\sigma_p$ (Figure 6), indeed the 2 most positive deviations are for the trisubstituted radicals, *tert*-butyl and trifluoromethyl; yet, of the 11 total trisubstituted radicals in Table 1, 3 actually show negative deviations. Inversely, the 2 most negative deviations are for disubstituted radicals, 1,2-dichloroethyl and 1,2,2,2-tetrafluoroethyl, not for monosubstituted ones; of the 11 total disubstituted radicals, 6 show negative deviations and 5 show positive deviations. Finally, for the 13 total monosubstituted radicals, 10 show negative deviations but 3 show positive deviations. While the averages of these deviations, 0.33, −0.07, and −0.21, do indeed fall in the order trisubstituted > disubstituted > monosubstituted, their standard deviations are large, ±0.45, ±0.51, and ±0.33, respectively, and overlapping. Hence, a "steric" effect related to the degree of substitution at the radical center does not appear to be a strong correlating factor.

Correlations with the Identity of the Halogen. There are 12 cases in Tables 1 and 2 for which the rate constants for chlorine and bromine transfer can be compared. As already surmised,[89] the ratio $k_{Br,298}/k_{Cl,298}$ is always greater than unity and ranges from 2.5 for the highly reactive *tert*-butyl to 155 for the relatively unreactive fluorodichloromethyl. A plot of log $k_{Br,298}$ vs log $k_{Cl,298}$ (r^2 = 0.952) has a slope of 0.66; i.e., the larger $k_{Br,298}$ is less sensitive to radical structure than the smaller $k_{Cl,298}$. A plot of log ($k_{Br,298}/k_{Cl,298}$) vs log $k_{Cl,298}$ (r^2 = 0.84) has a slope of −0.34; i.e., the selectivity decreases as the absolute reactivity increases. These are both intuitively satisfying conclusions. Unfortunately, a parallel comparison for iodine and chlorine transfer (Tables 1 and 3) is possible for only three cases; for ethyl, methyl, and trifluoromethyl, $k_{I,298}/k_{Cl,298}$ is 11, 54, and 54, respectively, each only modestly more selective than the corresponding $k_{Br,298}/k_{Cl,298}$ ratios of 6.6, 25, and 40, respectively. These limited data also are consistent with a saturation effect as the absolute reactivity increases. Finally, $k_{F,298}/k_{Cl,298}$ (Tables 1 and 4) is slightly less than unity for methyl (0.7) but slightly greater for ethyl (1.7) and trifluoromethyl (1.8).

Only for methyl, ethyl, and trifluoromethyl are rate constants for halogen transfer available in Tables 1−4 for all four halogens. To explore an enthalpy effect, we performed least-squares regressions of log $k_{X,298}(R^\bullet)$ for each of these three radicals vs (a) the overall reaction enthalpy, Δ_rH_{298}, (b) the strength of the bond being formed, $D°$(R−X), and (c) the strength of the bond being broken, $D°$(X−X) (note that the limited database of four halogens only allows two degrees of freedom). As Δ_rH_{298} becomes more negative, one would expect log $k_{X,298}$ to increase; i.e., the slope should be negative. In fact for all three radicals, the slopes of the (weak) correlations are positive. As $D°$(R−X) becomes larger (stronger bond formed), one would expect log $k_{X,298}$ to increase; i.e., the slope should be positive. In fact, the slopes of the (weak) correlations are all negative. Finally as $D°$(X−X) becomes larger (stronger bond broken), one would expect log $k_{X,298}$ to decrease; i.e., the slope should be negative. Only for this independent variable was the intuitive expectation of the sign of the slope realized, although the correlation is not strong (Table 8). (Note that this independent variable is known much more accurately than the other two (interrelated) ones.)

Table 8. Least-Squares Regressions of log $k_{X,298}$ for Radicals for Which $k_{X,298}$ Is Available for All Four Halogens[a]

	$D°$(X−X)		$\alpha(X_2)$[b]		$D°$(X−X) + $\alpha(X_2)$[c]	
R$^\bullet$	MUD[d]	r^2 [e]	MUD[d]	r^2 [e]	MUD[d]	r^2 [e]
$CH_3^\bullet$	0.69	0.15	0.29	0.82	0.28	0.85
$C_2H_5^\bullet$	0.31	0.36	0.19	0.69	0.14	0.85
$CF_3^\bullet$	0.62	0.25	0.38	0.67	0.33	0.76

[a] See text for sources of independent variables. [b] Mean polarizability of X_2. [c] Two-variable regression. [d] Mean unsigned deviation of log k_{exp} from log k_{calcd}. [e] Correlation coefficient of least-squares regression.

dx.doi.org/10.1021/jo2023075 | J. Org. Chem. 2012, 77, 2619−2636

To focus on the polar effect which places partial negative charge toward the halogen end of the precomplex and TS, we performed least-squares regressions of log $k_{X,298}(R^{\bullet})$ for each radical vs the Pauling electronegativity of the halogen atom, χ_P ($F \gg Cl > Br > I$),[93] the electron affinity of the halogen molecule, EA(X_2) ($F_2 \gg Br_2 \approx I_2 > Cl_2$),[93] and the electron affinity of the departing halogen atom, EA(X) ($Cl > F \approx Br > I$).[93] We note immediately the lack of correspondence with the reactivity order, which is $I_2 > Br_2 \gg Cl_2 \approx F_2$. Thus, as any one of these three parameters becomes more positive (better electron acceptor), one would expect log $k_{X,298}$ to increase; i.e., the slope should be positive. In fact for all three radicals for all three parameters, the slopes of the (weak) correlations are negative, and thus they do not offer a physically meaningful correlation. In contrast, following the suggestions above concerning a possible role for the mean polarizability of the halogen, $\alpha(X_2)$,[41,43,48,90] which increases in the "correct" order from F_2 to I_2 (1.21 to 4.61 to 6.99 to 12.4 Å^3),[90] we performed regressions of log $k_{X,298}$ vs α(X–X) for the three data sets. The correlation indicators were markedly improved over those for $D°$(X–X) (Table 8 and Figure 8).

Finally, we performed dual-variable regressions of log $k_{X,298}$ with $\alpha(X_2)$ paired with $D°$(X–X). Not surprisingly with only

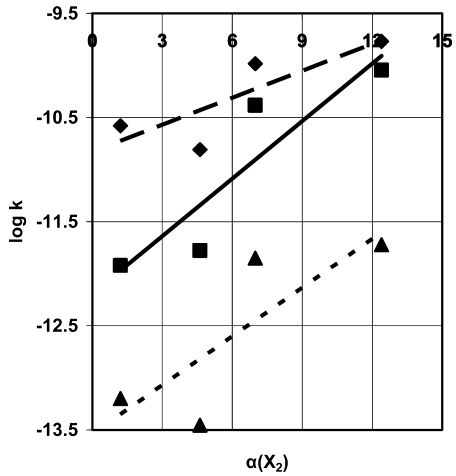

Figure 8. Dependence of log $k_{X,298}(R^{\bullet})$ (cm^3 molecule^{-1} s^{-1}) on $\alpha(X_2)$ (Å^3) for (■) methyl, (♦) ethyl, and (▲) trifluoromethyl. The lines are least-squares fits with $\alpha(X_2)$ increasing from X = F to Cl to Br to I (left to right).

one degree of freedom remaining, there was modest improvement over that with $\alpha(X_2)$ alone. These are shown in eq 4, Table 8, and Figure 9.

$$\log k_{X,298}(CH_3^{\bullet}) = -11.47 - 0.00358[D°(X–X)] + 0.176[\alpha(X_2)] \quad (4)$$

$$\log k_{X,298}(C_2H_5^{\bullet}) = -9.86 - 0.00482[D°(X–X)] + 0.0748[\alpha(X_2)]$$

$$\log k_{X,298}(CF_3\bullet) = -12.21 - 0.00660[D°(X–X)] + 0.141[\alpha(X_2)]$$

In each case the negative contribution to log $k_{X,298}$ from the $D°$(X–X) term varies only modestly in the order F ≈ I < Br < Cl while the offsetting positive contribution from the $\alpha(X_2)$ term increases sharply in the order F < Cl < Br < I. Hence, for example, the much faster iodine transfer compared with fluorine transfer does indeed appear to correlate with the much

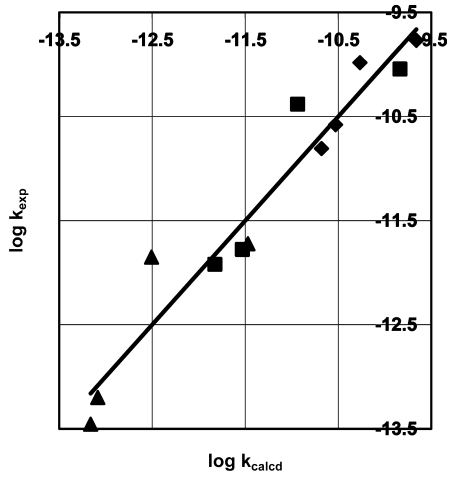

Figure 9. Comparison of log $k_{X,298}(R^{\bullet})$ (cm^3 molecule^{-1} s^{-1}) with that predicted from $D°$(X–X) (kJ/mol) and $\alpha(X_2)$ (Å^3) for (■) methyl, (♦) ethyl, and (▲) trifluoromethyl (eq 4). The line shows the ideal unit slope for perfect correlation. The identity of X for each point can be deduced from Figure 8.

greater polarizability of I_2, even though the I–I and F–F bonds are of comparable strength. (Regressions with $\alpha(X_2)$ paired instead with $\Delta_r H_{298}$ were slightly poorer than those paired with $D°$(X–X) and are not shown).

Global Correlation. Several combinations of independent variables could be considered in attempting to correlate the *combined* effects of alkyl radical structure and halogen identity on $k_{X,298}$. For simplicity we first limited ourselves to only two, and, considering the results from Tables 5–8, we chose $\sum\sigma_p$ and $\alpha(X_2)$, parameters which are available for all 60 data points (36 for Cl_2, 16 for Br_2, and 4 each for I_2 and F_2). The linear least-squares correlation is given in eq 5 with MUD = 0.59 log unit and r^2 = 0.82. Although the average deviation for the total set was of course 0, Figure 10 shows there was a tendency for overprediction of $k_{Cl,298}$ (average deviation of +0.31 log unit) and $k_{I,298}$ (+0.54 log unit) and under-prediction of $k_{Br,298}$ (−0.67 log unit) and $k_{F,298}$ (−0.65 log unit). Adding $D°$(X–X), also available for all cases, as a third variable gave eq 6 with MUD improved only slightly to 0.56 log unit and r^2 increased only slightly to 0.85. As can be seen from Figure 11, the tendency to overpredict $k_{Cl,298}$ was much improved (average deviation of +0.10 log unit) although that to overpredict $k_{I,298}$ was now somewhat greater (+0.77 log unit); meanwhile, the tendency to underpredict $k_{Br,298}$ was also somewhat improved (−0.50 log unit) and that to underpredict $k_{F,298}$ was reversed (+0.34 log unit). Finally, adding the quadratic dependence on $\sum\sigma_p$ to obtain eq 7 gave only minor further improvement to MUD = 0.53 log unit and r^2 = 0.86.

$$\log k_{X,298} = -(12.45 \pm 0.27) - (4.18 \pm 0.28)[\sum\sigma_p] + (0.189 \pm 0.043)[\alpha(X_2)] \quad (5)$$

$$\log k_{X,298} = -(9.57 \pm 0.86) - (4.08 \pm 0.26)[\sum\sigma_p] + (0.116 \pm 0.045)[\alpha(X_2])) - (0.0115 \pm 0.0033)[D°(X–X)] \quad (6)$$

dx.doi.org/10.1021/jo2023075 | J. Org. Chem. 2012, 77, 2619–2636

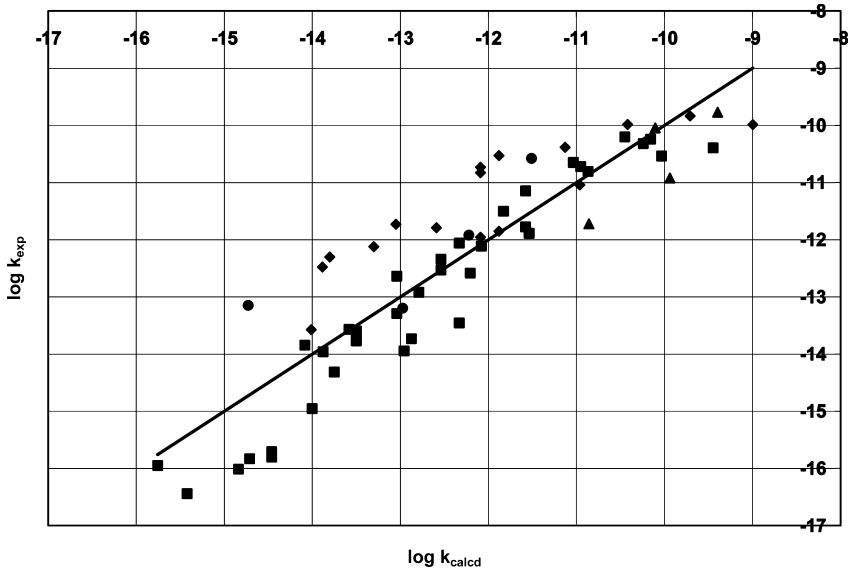

Figure 10. Comparison of log $k_{X,298}(R^{\bullet})$ (cm^3 $molecule^{-1}$ s^{-1}) with that predicted from $\sum\sigma_p$ and $\alpha(X_2)$ (Å^3) for (■) chlorine, (♦) bromine, (▲) iodine, and (●) fluorine (eq 5). The line shows the ideal unit slope for perfect correlation.

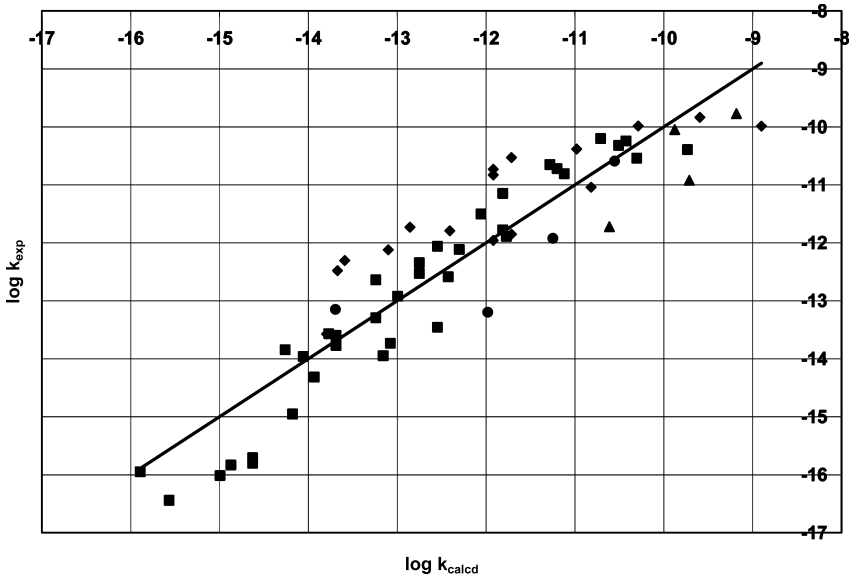

Figure 11. Comparison of log $k_{X,298}(R^{\bullet})$ (cm^3 $molecule^{-1}$ s^{-1}) with that predicted from $\sum\sigma_p$, $\alpha(X_2)$ (Å^3), and $D°$(X-X) (kJ/mol) for (■) chlorine, (♦) bromine, (▬) iodine, and (●) fluorine (eq 6). The line shows the ideal unit slope for perfect correlation.

$$\log k_{X,298} = -(9.65 \pm 0.83) - (3.54 \pm 0.36)[\sum\sigma_p] + (1.29 \pm 0.61)[\sum\sigma_p{}^2] + (0.115 \pm 0.043)[\alpha(X_2)] - (0.0105 \pm 0.0032)[D°(X{-}X)] \quad (7)$$

While these correlations are not nearly as good as the even broader ones for hydrogen transfer, e.g., that of Roberts,[81,82] it is likely that there is more experimental error in the database for halogen transfer than for hydrogen transfer. Thus eqs 5 and 6 set targets for both more extensive and improved data as well as improved correlation structures.

■ CONCLUSION

Experimental rate constants for the halogen transfer reaction ($R'_3C^{\bullet} + X_2 \rightarrow R'_3CX + X^{\bullet}$; X = F, Cl, Br, I) for trisubstituted alkyl radicals have been reviewed, and the characteristic occurrence of curved Arrhenius plots (some with minima) and negative activation energies is demonstrated. The viability of numerous potential independent variables for structure−reactivity correlation was explored. A modestly successful correlation of log k_X at 298 K has been achieved with the use of only two independent variables: $\sum\sigma_p$, the arithmetic sum of the Hammett σ_p constants for the substituents on the radical center, and $\alpha(X_2)$, the mean polarizability of the halogen. The mean unsigned deviation was 0.59 log unit for a span of 6.5 orders of magnitude in $k_{X,298}$. These independent variables support the dominant influence of a polar effect on the rate constant. It remains to be seen how much of the residual variance is the result of inaccuracies in the data compared with inadequacies in the correlation approach.

dx.doi.org/10.1021/jo2023075 | J. Org. Chem. 2012, 77, 2619−2636

■ ASSOCIATED CONTENT

Supporting Information

Figures S-1−S-5, giving Arrhenius plots of literature data for $CH_3^•$, $C_2H_5^•$, $R^•$ ($R^•$ = Me, Et, *i*-Pr, *t*-Bu), $Cl_xCH_{3-x}^•$, and $CH_3Cl_xCH_{2-x}^•$, and Table S-1, giving the values of the parameters used in the various regressions. This material is available free of charge via the Internet at http://pubs.acs.org.

■ AUTHOR INFORMATION

Corresponding Author

*Guest scientist. E-mail: poutsmaml@ornl.gov. Fax: 865-576-7956.

Notes

Notice: This manuscript has been authored by UT-Battelle, LLC, under Contract No. DE-AC05-00OR22725 with the U.S. Department of Energy. The United States Government retains and the publisher, by accepting the article for publication, acknowledges that the United States Government retains a nonexclusive, paid-up, irrevocable, worldwide license to publish or reproduce the published form of this manuscript, or allow others to do so, for United States Government purposes.
The authors declare no competing financial interest.

■ ACKNOWLEDGMENTS

This research was sponsored by the Division of Chemical Sciences, Geosciences and Biosciences, Office of Basic Energy Sciences, U.S. Department of Energy.

■ REFERENCES

(1) Slagle, I. R.; Gutman, D. *J. Am. Chem. Soc.* **1985**, *107*, 5342.
(2) Kovalenko, L. J.; Leone, S. R. *J. Chem. Phys.* **1984**, *80*, 3656.
(3) Nesbitt, D. J.; Leone, S. R. *J. Chem. Phys.* **1981**, *75*, 4949.
(4) Maricq, M. M.; Szente, J. J.; Hybl, J. D. *J. Phys. Chem. A* **1997**, *101*, 5155.
(5) Nelson, H. H.; McDonald, J. R. *J. Phys. Chem.* **1982**, *86*, 1242.
(6) Kaiser, E. W.; Wallington, T. J.; Andino, J. M. *Chem. Phys. Lett.* **1990**, *168*, 309.
(7) Kaiser, E. W.; Rimai, L.; Wallington, T. J. *J. Phys. Chem.* **1989**, *93*, 4094.
(8) Dobis, O.; Benson, S. W. *Z. Phys. Chem.* **2001**, *215*, 283.
(9) Dobis, O.; Benson, S. W. *J. Phys. Chem. A* **2000**, *104*, 5503.
(10) Eskola, A. J.; Timonen, R. S.; Marshall, P.; Chesnokov, E. N.; Krasnoperov, L. N. *J. Phys. Chem. A* **2008**, *112*, 7391.
(11) Timonen, R. S.; Gutman, D. *J. Phys. Chem.* **1986**, *90*, 2987.
(12) Eskola, A. J.; Lozovsky, V. A.; Timonen, R. S. *Int. J. Chem. Kinet.* **2007**, *39*, 614.
(13) Tyndall, G. S.; Orlando, J. J.; Wallington, T. J.; Dill, M.; Kaiser, E. W. *Int. J. Chem. Kinet.* **1997**, *29*, 43 and references therein.
(14) Lenhardt, T. M.; McDade, C. E.; Bayes, K. D. *J. Chem. Phys.* **1980**, *72*, 304.
(15) Kaiser, E. W.; Wallington, T. J.; Hurley, M. D. *Int. J. Chem. Kinet.* **1995**, *27*, 205.
(16) Caralp, F.; Lesclaux, R.; Dognon, A. M. *Chem. Phys. Lett.* **1986**, *129*, 433.
(17) Masanet, J.; Caralp, F.; Ley, L.; Lesclaux, R. *Chem. Phys.* **1992**, *160*, 383.
(18) Seetula, J. A.; Gutman, D.; Lightfoot, P. D.; Rayes, M. T.; Senkan., S. M. *J. Phys. Chem.* **1991**, *95*, 10688.
(19) Seetula, J. *J. Chem. Soc., Faraday Trans.* **1998**, *94*, 3561.
(20) Rissanen, M. P.; Eskola, A. J.; Timonen, R. S. *J. Phys. Chem. A* **2010**, *114*, 4805.
(21) DeMare, G. R.; Huybrechts, G. *Trans. Faraday Soc.* **1968**, *64*, 1311.
(22) Timonen, R. S.; Russell, J. J.; Gutman, D. *Int. J. Chem. Kinet.* **1986**, *18*, 1193.
(23) Kaiser, E. W. *Int. J. Chem. Kinet.* **1993**, *25*, 667.
(24) Maricq, M. M.; Szente, J. J.; Kaiser, E. W. *Chem. Phys. Lett.* **1992**, *197*, 149.
(25) Cullison, R. F.; Pogue, R. C.; White, M. L. *Int. J. Chem. Kinet.* **1973**, *5*, 415.
(26) DiLoreto, H. E.; Castellano, E. *J. Photochem.* **1987**, *38*, 65.
(27) Olbregts, J. *Int. J. Chem. Kinet.* **1979**, *11*, 117.
(28) Gillotay, D.; Olbregts., J. *Int. J. Chem. Kinet.* **1976**, *8*, 11.
(29) Ayscough, P. B.; Dainton, F. S.; Fleischfresser, B. E. *Trans. Faraday Soc.* **1966**, *62*, 1838.
(30) Knyazev, V. D.; Bencsura, A.; Dubinsky, I. A.; Gutman, D.; Melius, C. F.; Senkan, S. M. *J. Phys. Chem.* **1995**, *99*, 230.
(31) Butkovskaya, N. I.; Poulet, G.; LeBras, G. *J. Phys. Chem.* **1995**, *99*, 4536.
(32) Tyndall, G. S.; Orlando, J. J.; Kegley-Owen, C. S.; Wallington, T. J.; Hurley, M. D. *Int. J. Chem. Kinet.* **1999**, *31*, 776.
(33) Sehested, J.; Mogelberg, T.; Wallington, T. J.; Kaiser, E. W.; Nielsen, O. J. *J. Phys. Chem.* **1996**, *100*, 17218.
(34) Masaki, A.; Tsunashima, S.; Washida, N. *J. Phys. Chem.* **1995**, *99*, 13126.
(35) Kaiser, E. W.; Wallington, T. J.; Hurley, M. D. *J. Phys. Chem. A* **2009**, *113*, 2424.
(36) Kaiser, E. W.; Wallington, T. J.; Hurley, M. D. *J. Phys. Chem. A* **2010**, *114*, 343.
(37) Amphlett, J. C.; Whittle, E. *Trans. Faraday Soc.* **1966**, *62*, 1662.
(38) Skorobogatov, G. A.; Khripun, V. K.; Rebrova, A. G. *Kinet. Catal.* **2008**, *49*, 466. Pagsberg, P.; Jodkowski, J. T.; Ratajczak, E.; Sillesen, A. *Chem. Phys. Lett.* **1998**, *286*, 138.
(39) Timonen, R. S.; Russell, J. J.; Sarzynski, D.; Gutman, D. *J. Phys. Chem.* **1987**, *91*, 1873.
(40) IUPAC Subcommittee for Gas Kinetic Data Evaluation (http://www.iupac-kinetic.ch.cam.ac.uk); accessed July, 2011.
(41) Timonen, R. S.; Seetula, J. A.; Gutman, D. *J. Phys. Chem.* **1990**, *94*, 3005.
(42) Khamaganov, V.; Crowley, J. N. *Int. J. Chem. Kinet.* **2010**, *42*, 575.
(43) Timonen, R. S.; Seetula, J. A.; Niiranen, J.; Gutman, D. *J. Phys. Chem.* **1991**, *95*, 4009.
(44) Young, M. A.; Pimentel, G. C. *Int. J. Chem. Kinet.* **1991**, *23*, 58.
(45) Rossi, M. J.; Barker, J. R.; Golden, D. M. *J. Chem. Phys.* **1979**, *71*, 3722.
(46) Rossi, M. J.; Barker, J. R.; Golden, D. M. *Int. J. Chem. Kinet.* **1982**, *14*, 499.
(47) Hudgens, J. W.; Johnson, R. D. III; Timonen, R. S.; Seetula, J. A.; Gutman, D. *J. Phys. Chem.* **1991**, *95*, 4000.
(48) Timonen, R. S.; Seetula, J. A.; Gutman, D. *J. Phys. Chem.* **1993**, *97*, 8217.
(49) Slagle, I. R.; Yamada, F.; Gutman, D. *J. Am. Chem. Soc.* **1981**, *103*, 149.
(50) Fettis, G. C.; Trotman-Dickenson, A. F. *J. Chem. Soc.* **1961**, 3037.
(51) Seakins, P. W.; Pilling, M. J.; Niranen, J. T.; Gutman, D.; Krasnoperov, L. N. *J. Phys. Chem.* **1992**, *96*, 9847.
(52) Seetula, J. *Phys. Chem. Chem. Phys.* **2002**, *4*, 455.
(53) Williams, R. R.; Ogg, R. A. Jr. *J. Chem. Phys.* **1947**, *15*, 696.
(54) Seetula, J. A.; Russell, J. J.; Gutman, D. *J. Am. Chem. Soc.* **1990**, *112*, 1347.
(55) O'Neal, E.; Benson, S. W. *J. Chem. Phys.* **1962**, *36*, 2196.
(56) Flowers, M. C.; Benson, S. W. *J. Chem. Phys.* **1963**, *38*, 882.
(57) Sullivan, J. H. *J. Phys. Chem.* **1961**, *65*, 722.
(58) Ogg, R. A. Jr. *J. Am. Chem. Soc.* **1934**, *56*, 526.
(59) Hunter, T. F.; Kristjansson, K. S. *J. Chem. Soc., Faraday Trans 2* **1982**, *78*, 2067.
(60) Hartley, D. B.; Benson, S. W. *J. Chem. Phys.* **1963**, *39*, 132.
(61) Nicholas, J. E.; Vaghjiana, G. *J. Chem. Soc., Faraday Trans 2* **1986**, *82*, 1945.
(62) Christie, M. I.; Frost, J. S. *Trans. Faraday Soc.* **1965**, *61*, 468.

(63) NIST Chemical Kinetics Database, Standard Reference Database 17, Version 7.0 (Web Version), Release 1.6.3 (http://kinetics.nist.gov); accessed July, 2011.
(64) Hayes, D. M.; Strong, R. L. *J. Phys. Chem.* **1986**, *90*, 6305.
(65) Tucker, B. G.; Whittle, E. *Trans. Faraday Soc.* **1965**, *61*, 866.
(66) Amphlett, J. C.; Macauley, L. J. *Can. J. Chem.* **1976**, *54*, 1234.
(67) Skorobogatov, G. A.; Dymov, B. P.; Khripun, V. K. *Kinet. Catal.* **1991**, *32*, 220. Skorobogatov, G. A.; Dymov, B. P.; Tedeev, R. S. *J. Gen. Chem. USSR* **1991**, *61*, 158.
(68) Jenkin, M. E.; Murrells, T. P.; Shalliker, S. J.; Hayman, G. D. *J. Chem. Soc., Faraday Trans.* **1993**, *89*, 433.
(69) Moore, C. M.; Smith, I. W. M.; Stewart, D. W. A. *Int. J. Chem. Kinet.* **1994**, *26*, 813.
(70) Seeger, C.; Rotzoll, G.; Lubbert, A.; Schugerl, K. *Int. J. Chem. Kinet.* **1981**, *13*, 39.
(71) Gyul'bekyan, Z. K.; Vedeneev, V. I.; Gorban', N. I.; Sarkisov, O. M. *Kinet. Catal.* **1976**, *17*, 740.
(72) Teitel'boim, M. A.; Vedeneev, V. I. *Kinet. Catal.* **1985**, *26*, 1119.
(73) Plumb, I. C.; Ryan, K. R. *Plasma Chem. Plasma Process.* **1986**, *6*, 11.
(74) Donahue, N. M. *Chem. Rev.* **2003**, *103*, 4593.
(75) Tirtowidjojo, M. M.; Colegrove, B. T.; Durant, J. L. Jr. *Ind. Eng. Chem. Res.* **1995**, *34*, 4202.
(76) Lee, J.; Bozzelli, J. W.; Sawerysyn, J. P. *Int. J. Chem. Kinet.* **2000**, *32*, 548.
(77) Drougas, E.; Papayannis, D. K.; Kosmas, A. M. *J. Phys. Chem. A* **2002**, *106*, 6339.
(78) Drougas, E.; Papayannis, D. K.; Kosmas, A. M. *THEOCHEM* **2003**, *623*, 211.
(79) Poutsma, M. L. *J. Anal. Appl. Pyrol.* **2000**, *54*, 5.
(80) Isborn, C.; Hrovat, D. A.; Borden, W. T.; Mayer, J. M.; Carpenter, B. K. *J. Am. Chem. Soc.* **2005**, *127*, 5794.
(81) Roberts, B. P.; Steel, A. J. *J. Chem. Soc., Perkin Trans 2* **1994**, 2155.
(82) Roberts, B. P. *J. Chem. Soc., Perkin Trans. 2* **1996**, 2719.
(83) Zavitsas, A. A. *J. Am. Chem. Soc.* **1972**, *94*, 2779. Zavitsas, A. A. *J. Am. Chem. Soc.* **1975**, *97*, 2757.
(84) Zavitsas, A. A.; Chatgilialoglu, C. *J. Am. Chem. Soc.* **1995**, *117*, 10645.
(85) Zavitsas., A. A. *J. Chem. Soc., Perkin Trans. 2* **1996**, 391.
(86) Matsunaga, N.; Rogers, D. W.; Zavitsas, A. A. *J. Org. Chem.* **2003**, *68*, 3158. Coote, M. L.; Lin, C. Y.; Beckwith, A. L. J.; Zavitsas, A. A. *Phys. Chem. Chem. Phys.* **2010**, *12*, 9597.
(87) Thomas, T. D. *J. Am. Chem. Soc.* **1970**, *92*, 4184.
(88) Seetula, J. A.; Gutman, D. *J. Phys. Chem.* **1991**, *95*, 3626.
(89) Evans, B. S.; Whittle, E. *Int. J. Chem. Kinet.* **1978**, *10*, 745.
(90) Krech, R. H.; McFadden, D. L. *J. Am. Chem. Soc.* **1977**, *99*, 8402.
(91) Mayer, J. M. *Acc. Chem. Res.* **2011**, *44*, 36.
(92) Luo, Y. R. In *CRC Handbook of Chemistry and Physics, Internet Version 2011*, 91st ed.; Lide, D. R., Ed.; CRC Press: Boca Raton, FL, 2011; Section 9 (Bond Dissociation Energies) (http://www.hbcpnetbase.com; accessed July 2011).
(93) *CRC Handbook of Chemistry and Physics, Internet Version 2011*, 91st ed.; Lide, D. R., Ed.; CRC Press: Boca Raton, FL, 2011; Sections 9 (Electronegativities) and 10 (Electron Affinities) (http://www.hbcpnetbase.com; accessed July 2011).
(94) Pearson, R. G. *J. Am. Chem. Soc.* **1988**, *110*, 7684.
(95) NIST Chemistry Webbook, Standard Reference Database 69 (http://webbook.nist.gov/chemistry); accessed July 2011.
(96) Hansch, C.; Leo, A.; Taft, R. W. *Chem. Rev.* **1991**, *91*, 165.
(97) Alfassi, Z. B.; Benson, S. W. *Int. J. Chem. Kinet.* **1973**, *5*, 879.